Int J Earth Sci (Geol Rundsch) (2017) 106:355–375
DOI 10.1007/s00531-016-1323-2

ORIGINAL PAPER

Is the Paleoproterozoic Jiao-Liao-Ji Belt (North China Craton) a rift?

Zhuang Li[1] · Bin Chen[2] · Chunjing Wei[1]

Received: 16 January 2016 / Accepted: 31 March 2016 / Published online: 12 April 2016

Abstract As a typical example of the Paleoproterozoic crust in the Eastern Block of the North China Craton, the Paleoproterozoic Jiao-Liao-Ji Belt consists principally of the Liaohe Group (and its equivalents), Liaoji granites and mafic intrusions. Previous studies indicate that the evolution of the Jiao-Liao-Ji Belt has been mainly attributed to the opening and closing of an intracontinental rift along the eastern continental margin of the North China Craton. Here we synthesize the Paleoproterozoic magmatism, sedimentation, metamorphism and metallogeny against the rift model and propose a process of arc-continent collision between the northern Longgang and the southern Nangrim Blocks. This conclusion is consistent with the observations, including that (a) the 2.0- to 2.2-Ga magmatism shows a typical subalkaline series, rather than a bimodal distribution, since the mafic rocks mostly have arc affinities and the acidic–intermediate rocks belong to the calc-alkaline series; (b) the main source of the 1.9- to 2.0-Ga sedimentary rocks is the Paleoproterozoic arc materials, indicating a fore-arc or back-arc basin setting; (c) a couple of big borate deposits occur in the boron-rich volcanic rocks that were formed in convergent continental margins; (d) the North and South Liaohe Groups show different rock associations and metamorphic histories (P–T paths); and (e) the Nangrim and Longgang Blocks vary in lithological units, geochronology and metamorphic features. Thus, an arc-continent collision tectonic scenario for the Paleoproterozoic Jiao-Liao-Ji Belt is involved: (a) a southward subduction in the period 2.0–2.2 Ga; (b) sedimentation during the period 1.9–2.0 Ga; (c) arc-continent collision at ca. 1.9 Ga; and (d) post-collisional extension at 1.82–1.87 Ga, marking the end of the Paleoproterozoic tectonothermal event.

Keywords Paleoproterozoic · Jiao-Liao-Ji Belt · North China Craton · Tectonic evolution

✉ Zhuang Li
lizhuangcc@pku.edu.cn

[1] The Key Laboratory of Orogenic Belts and Crustal Evolution, Ministry of Education, School of Earth and Space Sciences, Peking University, Beijing 100871, People's Republic of China

[2] School of Resources and Environmental Engineering, Hefei University of Technology, Hefei, Anhui 230009, People's Republic of China

Introduction

The Paleoproterozoic marks an important period in Earth history as it witnessed a transition from Archean planar tectonic systems to Post-Archean linear ones (Smith 1992; Windley 1992). Three Paleoproterozoic mobile belts have been recognized on the North China Craton (NCC). They are the Khondalite Belt (also known as the Inner Mongolia Suture Zone), the Trans-North China Orogen and the Jiao-Liao-Ji Belt (JLJB), based mainly on the field-based structural, metamorphic, geochemical, geochronological and geophysical investigations on these belts (Fig. 1; Zhao and Zhai 2013, and references therein). Although a consensus has not been reached in the subdivision and formation of the NCC (Zhai and Santosh 2011, 2013; Zhao and Zhai 2013), there is an increasing agreement that the Khondalite Belt resulted from amalgamation of the Yinshan and Ordos Blocks, forming the Western Block at ca. 1.92–1.95 Ga (Peng et al. 2010, 2011; Santosh et al. 2007; Santosh 2010; Xia et al. 2006; Zhao et al. 2005, 2010), and the Trans-North China Orogen was formed by collision between the Western and Eastern Blocks at ca. 1.85 Ga (e.g., Wan et al. 2006b; Zhai and Santosh 2011, 2013; Zhao and Zhai 2013;

Zhao et al. 2005, 2010). However, the tectonic nature and evolution of the JLJB remain matters of debate (Li et al. 2011). Most scientists believe that the JLJB was formed by closure of an intracontinental rift (Hao et al. 2004; Li and Zhao 2007; Li et al. 2001, 2005, 2006, 2011, 2012; Luo et al. 2004, 2008; Tam et al. 2011, 2012a, b), mainly based on the occurrence of bimodal volcanic rocks, the existence of voluminous pre-tectonic A-type granite plutons (Peng and Palmer 1995, 2002; Sun et al. 1993, 1996; Zhang and Yang 1988), the low-P and anticlockwise P–T paths of the metamorphic rocks of the Liaohe Group (He and Ye 1998; Lu 1996), and the similar Archean basement rocks occurred at both margins of the JLJB (Zhang and Yang 1988; Lu et al. 2004a, 2005, 2006). Some others, however, suggest that it is a Paleoproterozoic arc-continent collisional belt (Bai 1993; Li and Chen 2014; Li et al. 2015a, b, 2016a; Lu et al. 2006; Meng et al. 2014; Wang et al. 2011a, b; Yuan et al. 2015). In order to resolve the controversial idea, we present an overview of the recent progress in the study of the Paleoproterozoic magmatism, sedimentation, metamorphism and metallogeny in the Liaodong Peninsula and adjacent regions, which will provide new insights into the tectonic evolution of the JLJB.

Geological setting

The NCC is one of the oldest continental nuclei on Earth (Liu et al. 1992; Wan et al. 2005, 2012), being bounded to the north by the Central Asian Orogenic Belt and to the south by the Qinling–Dabie–Su–Lu ultrahigh-pressure metamorphic belt (Fig. 1a; Li et al. 2016a; Wan et al. 2005). The Liaodong Peninsula is located on the northeastern margin of NCC (Fig. 1b; Li et al. 2014a, b).

The late Archean–Paleoproterozoic basement of the Liaodong Peninsula, overlain by unmetamorphosed Mesoproterozoic–Cenozoic cover rocks, can be subdivided into three tectonic units, including the Archean Longgang Block, the Archean Nangrim Block and the Paleoproterozoic JLJB in between (Fig. 2; Li and Chen 2014; Li et al. 2016b; Zhao and Zhai 2013; Zhao et al. 2005). The Archean basement mainly consists of high-grade metamorphic terrane and the

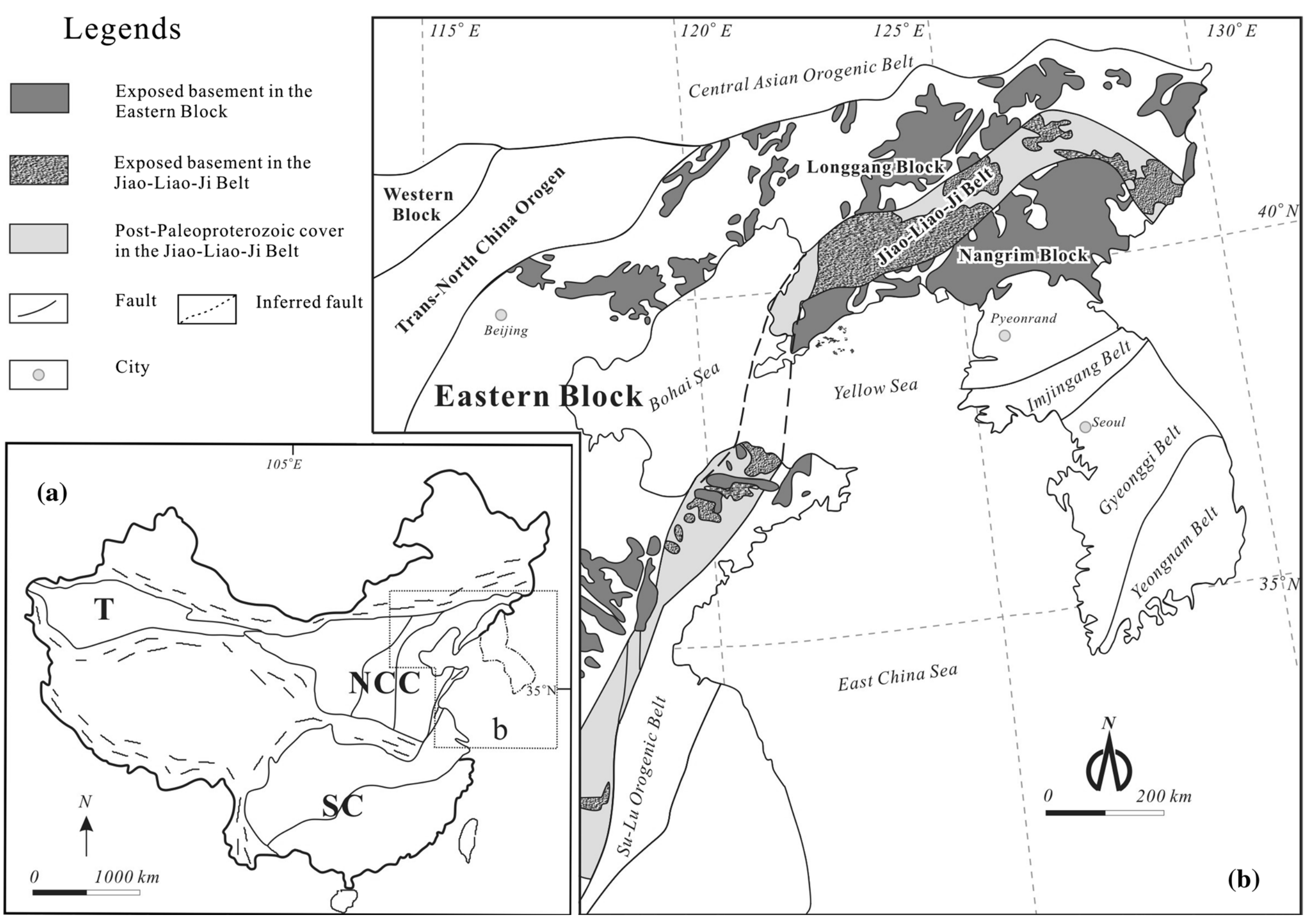

Fig. 1 Schematic *map* showing *a* the location of the North China Craton, in China (SC: South China, T: Tarim) and *b* the distribution of the Jiao-Liao-Ji Belt in the eastern part of the North China Craton (modified after Zhao et al. 2005)

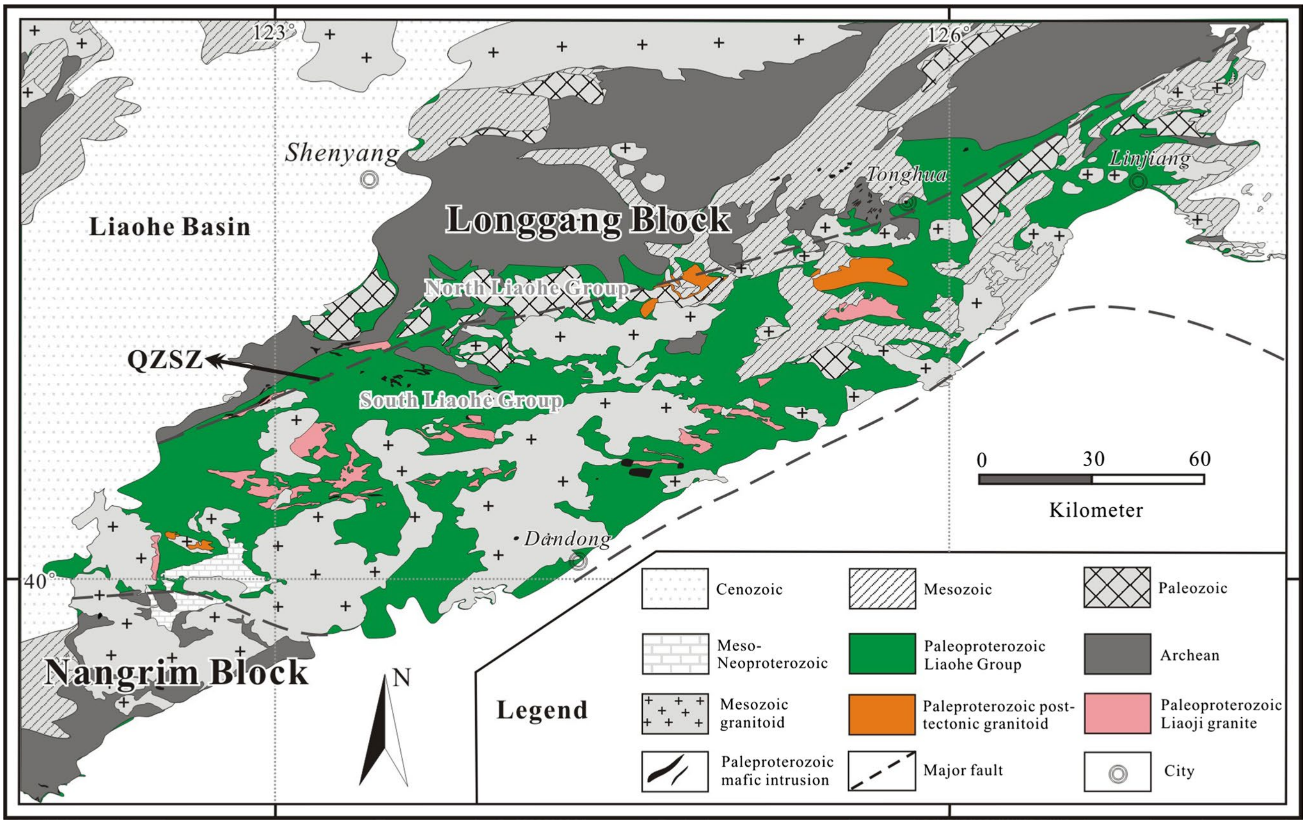

Fig. 2 Geological *map* of the Archean–Paleoproterozoic basement and post-Paleoproterozoic cover in the Liaodong Peninsula. QZSZ, Qinglongshan–Zaoerling shear zone (modified after Li et al. 2005, 2011, 2016a and Pei et al. 2011)

middle- to lower-grade granite–greenstone belt (Lin et al. 1997; Wang et al. 2011a, b). The Paleoproterozoic rocks, which unconformably overlie the Archean basement, are composed of volcano-sedimentary successions and granite–mafic intrusions that were deformed and metamorphosed to greenschist–amphibolite facies at ca. 1.9 Ga (Fig. 2; Li and Chen 2014; Li and Zhao 2007; Li et al. 2005, 2006, 2011, 2015a, b; Lu et al. 2004a, b, 2006; Luo et al. 2004, 2008; Meng et al. 2014; Yuan et al. 2015). The volcano-sedimentary successions are called the Liaohe Group in the Liaodong Peninsula (the Macheonayeong Group in North Korea, the Laoling and Ji'an Groups in southern Jilin, the Fenzishan and Jingshan Groups in Shandong Peninsula, Li et al. 2011; Zhao and Zhai 2013; Zhao et al. 2005). The Liaohe Group is divided into two parts (i.e., South and North Liaohe Groups) by the Qinglongshan–Zaoerling shear zone (QZSZ; Li et al. 2005, 2011). The South Liaohe Group is composed of more volcanic rocks than the North Liaohe Group (Bai 1993; Lu 1996; Zhang and Yang 1988). The Liaohe Group consists of three rock units, with (1) an arkose- and volcanic-rich sequence in the lower part (the Langzishan, Lieryu and Gaojiayu Formations), (2) a carbonate-rich sequence in the middle (the Dashiqiao Formation) and (3) a pelitic sequence in the upper part (the Gaixian Formation) (Li et al. 2014a, b, 2015a, b). Many ore deposits occur in the Paleoproterozoic Liaohe Group, including the world-class magnesite and borate deposits, and Pb–Zn–Au deposits. The giant Dashiqiao magnesite deposit was hosted in the Dashiqiao Formation, notable for its thick and pure ore-body (Tang et al. 2009). The boron ore-bodies were hosted in fine-grained felsic gneiss of the Lieryu Formation (Peng and Palmer 1995, 2002). In addition, many Pb–Zn ore deposits and Cu–Au ores are discovered in the Gaojiayu Formation (e.g., Zhai and Santosh 2013). Paleoproterozoic granite–mafic intrusions can be divided into two episodes, 2.0–2.2 and 1.82–1.87 Ga (Li and Zhao 2007; Li et al. 2015b; Lu et al. 2006), which will be discussed in details in later section.

Subsequently, the Liaodong Peninsula was covered by thick Meso–Neoproterozoic and Paleozoic sediment sequences (Zhang et al. 2009, 2012). The Meso–Neoproterozoic unmetamorphosed volcano-sedimentary successions lie in disconformable contact with the underlying Archean–Paleoproterozoic basement, including the Changcheng, Jixian and Qingbaikou systems from the bottom to the top (Li et al. 1995; Zhao et al. 2005). Each system contacts disconformably with the underlying system, and the formations within each system are in conformable contact.

The Early Paleozoic strata are represented by the Cambrian–Middle Ordovician carbonate deposits. The late Carboniferous to Early Permian marine and terrestrial sequence is characterized by carbonates and coal-bearing rocks, overlying by late Permian–Triassic red beds and conglomerates. The Jurassic strata are absent in the Liaodong Peninsula (LBGMR 1989; Wu et al. 2007). The Early Cretaceous strata contain a significant amount of volcanic rocks, with sedimentary rocks that contain abundant fossils (Gao et al. 2004; Wang et al. 2001). They are covered by late Cretaceous to Cenozoic sediments with widely distributed Cenozoic basalts (Meng 2003; Wu et al. 2007). In addition, Mesozoic granitoids are widely distributed throughout the Liaodong Peninsula (Fig. 2; Li et al. 2014a).

The spatial–temporal distribution and lithology of the Paleoproterozoic rocks

Previous studies indicated that the Paleoproterozoic rocks were widely distributed throughout the Liaodong Peninsula, mainly based on their relation with the country rocks in lithostratigraphy or ages by whole-rock K–Ar dating (1800–2300 Ma; LBGMR 1989; Zhang and Yang 1988). However, recently the high-precision dating reveals that the Paleoproterozoic rocks were not as widely distributed as previously thought (Miao et al. 2010), and some were even formed in the Phanerozoic (Li et al. 2014a; Miao et al. 2010; Pei et al. 2011). Integrating some unpublished data with reliable studies on the geochronology, we can subdivide the evolution of the Liaodong Peninsula into the following episodes: 2.0–2.2 Ga magmatism, 1.9–2.0 Ga sedimentation, ca. 1.9 Ga metamorphism and 1.82–1.87 Ga post-tectonic magmatism (Table 1; Fig. 3). A brief review of the events in each period will be presented in later sections.

Magmatism event (2.0–2.2 Ga)

The 2.0- to 2.2-Ga magmatism is exhibited by the volcanic rocks in the Lieryu Formation and a large amount of foliated granite–mafic intrusions. (a) In the previous sections, we have mentioned that more volcanic rocks of the South Liaohe Group were recognized than those of the North Liaohe Group (Bai 1993; Lu 1996; Zhang and Yang 1988). Zircon grains from the metamorphosed rhyolites and andesites display striped absorption and oscillatory growth zoning and high Th/U ratios (mostly >0.3, 0.42 on average), indicating a magma origin. U–Pb isotopic dating using the SHRIMP and LA-ICP-MS methods on zircons from the metamorphosed volcanic rocks reveals that they were formed at ca. 2.1–2.2 Ga (Chen et al. 2016; Li and Chen 2014; Li et al. 2015a; Liu et al. 2012; Wan et al. 2006a; Zhang et al. 2010). Commonly, it is difficult to obtain enough magmatic zircons from basalts for dating the protolith ages. These rocks were not well dated, but some of the basalts showed conformable contact with the felsic volcanic rocks, so we regarded them coeval (2.1–2.2 Ga; detailed description of contact relationship refers to Li and Chen 2014; Li et al. 2015a). (b) Similar to distribution of the volcanic rocks, foliated granite intrusions, termed as Liaoji granites, are mainly exposed in the south. Clear oscillatory growth zoning and high Th/U ratios (mostly >0.4, 0.48 on average) of the zircon grains from the Liaoji granites indicate a magma origin. U–Pb isotopic dating using the SHRIMP and LA-ICP-MS methods on zircons from the Liaoji granites reveals that they were mainly emplaced at 2.1–2.2 Ga (Chen et al. 2016; Li and Zhao 2007; Yang et al. 2015a). Conspicuously, the eruption age of the volcanism is comparable to those of the Liaoji granites fixed at 2.1–2.2 Ga. Therefore, it is inconsistent with a previous model that the Paleoproterozoic Liaoji granites were considered as the basement rocks of the Liaohe Group volcano-sedimentary rocks (Li and Zhao 2007; Li et al. 2011; Lu et al. 2004a, 2005, 2006; Luo et al. 2004, 2008) and, rather, suggest a synchronism for the two rock units (Li and Chen 2014; Li et al. 2015a). (c) The mafic rocks occur mostly as dykes or intrusions, such as those exposed at Liaoyang (Meng et al. 2014) and Guoguang (Yuan et al. 2015). The zircons from the mafic dykes or intrusions show weak internal texture, high U concentration and Th/U ratios (mostly >0.3, 0.35 on average), reminiscent of those with a typical mafic magmatic origin (Baines et al. 2009; Koglin et al. 2009). U–Pb isotopic dating using the SHRIMP and LA-ICP-MS methods on zircons reveals that they were mainly formed at 2.1–2.2 Ga (Meng et al. 2014; Yuan et al. 2015). In addition, it is worth to note that zircons with the ages of 2.0–2.1 Ga have been found in several Paleoproterozoic Liaoji granites and meta-mafic dykes (Table 1; Dong et al. 2012; Li et al. 2006; Wang et al. 2011a, b; Yu et al. 2007).

In summary, the 2.0- to 2.2-Ga volcanic rocks and foliated granite–mafic intrusions constitute a significant giant Paleoproterozoic igneous event in the Liaodong Peninsula (Fig. 3).

Sedimentation event (1.9–2.0 Ga)

As mentioned before, the Liaohe Group can be divided into several formations. The lowermost Langzishan Formation, unconformably overlying the Archean Anshan Complex, is only present in the North Liaohe Group and is composed of basal conglomerate-bearing quartzites, transitional upward to chlorite–sericite quartz schists, phyllites, garnet-bearing mica schists, minor

Table 1 Representative geochronological data for the Paleoproterozoic rocks in the Liaodong Peninsula, Jiao-Liao-Ji Belt

No.	Samples	Location (GPS)	Lithologies	Formations/intrusions	Ages (Ma)	Methods	Interpretations	References
2.0–2.2 Ga magmatism event								
Volcanic rock								
1	J1	Liaoning Province	Meta-volcanic rock	Lieryu Formation	2093 ± 22	SGDZ	Crystallization age	Jiang (1987)
2	J2	Liaoning Province	Meta-volcanic rock	Lieryu Formation	2053 +69/−67	SGDZ	Crystallization age	Jiang (1987)
3	B1	Liaoning Province	Amphibolite	Lieryu Formation	2193 ± 30	Sm–Nd	Crystallization age	Bai (1993)
4	B2	Liaoning Province	Amphibolite	Lieryu Formation	2063 ± 38	Sm–Nd	Crystallization age	Bai (1993)
5	K86243-7	Liaoning Province	Amphibolite	Lieryu Formation	2110 ± 60	Sm–Nd	Crystallization age	Sun et al. (1993)
6	Y006-1	41°29′32″N, 125°53′49″E	Diopside-bearing gneiss	Ji'an Group	2103 ± 18 ($n = 54$)	SHRIMP	Crystallization age	Lu et al. (2006)
7	Y009	41°18′16″N, 125°59′47″E	Garnet-bearing gneiss	Ji'an Group	1981 ± 13 ($n = 72$)	SHRIMP	Crystallization age	Lu et al. (2006)
8	LD0106-1	Dashiqiao area	Fine-grained biotite gneiss	Lieryu Formation	2179 ± 8 ($n = 12$)	SHRIMP	Crystallization age	Wan et al. (2006a, b)
9	N02	Houxianyu boron deposit	Hyalotourmalite	Lieryu Formation	2175 ± 6 ($n = 13$)	SHRIMP	Crystallization age	Liu et al. (2012)
10	N13	Houxianyu boron deposit	Hyalotourmalite	Lieryu Formation	2175 ± 5 ($n = 15$)	SHRIMP	Crystallization age	Liu et al. (2012)
11	N14	Houxianyu boron deposit	Hyalotourmalite	Lieryu Formation	2171 ± 9 ($n = 6$)	SHRIMP	Crystallization age	Liu et al. (2012)
12	DZ78-1	Yanggoumen Country	Amphibolite	Dashiqiao Formation	2161 ± 45 ($n = 4$)	LA-ICP-MS	Crystallization age	Meng et al. (2014)
13	LZ02-1	40°32′24″N, 122°43′45″E	Fine-grained gneiss	Lieryu Formation	2158 ± 23 ($n = 29$)	LA-ICP-MS	Crystallization age	Li and Chen (2014)
14	LZ04-1	40°32′24″N, 122°43′45″E	Fine-grained gneiss	Lieryu Formation	2172 ± 8 ($n = 24$)	LA-ICP-MS	Crystallization age	Li and Chen (2014)
15	LZ19-1	40°32′24″N, 122°43′45″E	Fine-grained gneiss	Lieryu Formation	2179 ± 8 ($n = 19$)	LA-ICP-MS	Crystallization age	Li and Chen (2014)
16	LZ3	40°32′24″N, 122°43′45″E	Fine-grained gneiss	Lieryu Formation	2201 ± 5 ($n = 27$)	LA-ICP-MS	Crystallization age	Li et al. (2015a)
17	HX35	40°21′25″N, 122°55′27″E	Meta-andesite	Lieryu Formation	2195 ± 6 ($n = 18$)	LA-ICP-MS	Crystallization age	Chen et al. (2016)
18	HX33	40°21′25″N, 122°55′27″E	Meta-andesite	Lieryu Formation	2200 ± 8 ($n = 24$)	LA-ICP-MS	Crystallization age	Chen et al. (2016)
Laioji Granite								
19	K86	Kuandian City	Granite	Kuandian Pluton	2140 ± 50	SGDZ	Crystallization age	Sun et al. (1993)
20	FW10-327	40°31′28″N, 122°47′54″E	Tourmaline muscovite granite	Hupiyu Pluton	2161 ± 12 ($n = 30$)	LA-ICP-MS	Crystallization age	Lu et al. (2004a)
21	Lu1065	41°23′39″N, 125°55′38″E	Syenogranite	Qianzhuogou Pluton	2173 ± 20 ($n = 11$)	LA-ICP-MS	Crystallization age	Lu et al. (2004a)
22	Lu0007	41°24′18″N, 125°36′37″E	Syenogranite	Qianzhuogou Pluton	2164 ± 8 ($n = 11$)	SHRIMP	Crystallization age	Lu et al. (2004a)
23	LD9822	Dashiqiao area	Biotite granite	Pailou Pluton	2173 ± 4 ($n = 10$)	SHRIMP	Crystallization age	Wan et al. (2006a, b)
24	LJ010	Xiaoxicha Village	Magnetite monzogranitic gneiss	Laoheishan Pluton	2166 ± 14 ($n = 14$)	SHRIMP	Crystallization age	Li and Zhao (2007)

Table 1 continued

No.	Samples	Location (GPS)	Lithologies	Formations/ intrusions	Ages (Ma)	Methods	Interpretations	References
25	LJ035	Moguling, Fengcheng City	Magnetite monzogranitic gneiss	Jiguangshan Pluton	2175 ± 13 ($n = 14$)	SHRIMP	Crystallization age	Li and Zhao (2007)
26	LJ056	Mafeng Town, Haicheng City	Magnetite monzogranitic gneiss	Mafeng Pluton	2176 ± 11 ($n = 7$)	SHRIMP	Crystallization age	Li and Zhao (2007)
27	LJ040	Zhenggou, Liaoning	Hornblende monzongranitic gneiss	Dafangsheng Pluton	2143 ± 17 ($n = 12$)	SHRIMP	Crystallization age	Li and Zhao (2007)
28	LJ044	Fujiapuzi, Hadabei Town	Biotite monzogranitic gneiss	Hupiyu Pluton	2150 ± 17 ($n = 13$)	SHRIMP	Crystallization age	Li and Zhao (2007)
29	HD-2	Hadabei Town	Biotite monzogranitic gneiss	Hadabei Pluton	2173 ± 20 ($n = 30$)	LA-ICP-MS	Crystallization age	Yang et al. (2015a)
30	SM-1	Simenzi Town	Hornblende monzongranitic gneiss	Simenzi Pluton	2203 ± 20 ($n = 18$)	LA-ICP-MS	Crystallization age	Yang et al. (2015a)
31	HP-1	Fujiapuzi, Hadabei Town	Biotite monzogranitic gneiss	Hupiyu Pluton	2159 ± 19 ($n = 18$)	LA-ICP-MS	Crystallization age	Yang et al. (2015a)
32	HPX 1	40°25′15″N, 122°35′22″E	Biotite monzogranitic gneiss	Hupiyu Pluton	2215 ± 3 ($n = 19$)	LA-ICP-MS	Crystallization age	Chen et al. (2016)
Mafic intrusion								
33	Y1	Mafeng Town	Meta-gabbro	Dyke	2059 ± 22 ($n = 16$)	LA-ICP-MS	Crystallization age	Yu et al. (2007)
34	09JL29	Mamajie Country	Meta-diabase	Dyke	2080 ($n = 3$)	SHRIMP	Crystallization age	Wang et al. (2011a, b)
35	A1102	Hanjiayu Town	Meta-gabbro	Dyke	2110 ± 31 ($n = 2$)	SHRIMP	Crystallization age	Dong et al. (2012)
36	DZ91-1	Mafeng Town	Meta-diabase	Dyke	2161 ± 12 ($n = 22$)	LA-ICP-MS	Crystallization age	Meng et al. (2014)
37	DZ73-1	Daxingtun Country	Meta-gabbro	Intrusion	2159 ± 12 ($n = 14$)	LA-ICP-MS	Crystallization age	Meng et al. (2014)
38	DZ85-1	Tianshui Town	Meta-gabbro	Intrusion	2157 ± 17 ($n = 6$)	LA-ICP-MS	Crystallization age	Meng et al. (2014)
39	DZ74-1	Xiabahui Town	Meta-gabbro	Intrusion	2144 ± 16 ($n = 24$)	LA-ICP-MS	Crystallization age	Meng et al. (2014)
40	YK12-1-4	Haicheng	Meta-gabbro	Intrusion	2127 ± 6 ($n = 16$)	CAMECA	Crystallization age	Yuan et al. (2015)
1.9–2.0 Ga sedimentation event (n = 1042)								
41	02L095-1	40°51.763′N, 122°55.849′E	Plagioclase-quartz schist	Langzishan Formation	2027–2240	LA-ICP-MS	Detrital zircon age	Luo et al. (2004)
42	02L095-2	40°51.763′N, 122°55.850′E	Pelitic schist	Langzishan Formation		LA-ICP-MS	Detrital zircon age	Luo et al. (2004)
43	LZ03-1	40°32′24″N, 122°43′45″E	Mica schist	Lieryu Formation	1987–2217	LA-ICP-MS	Detrital zircon age	Li et al. (2015b)
44	04L045-1	40°23′41″N, 122°55′35″E	Fine-grained biotite gneiss	Lieryu Formation		LA-ICP-MS	Detrital zircon age	Luo et al. (2008)
45	04L023-1	40°55.102′N, 123°10.769′E	Banded biotite plagioclase gneiss	Lieryu Formation		LA-ICP-MS	Detrital zircon age	Luo et al. (2008)
46	04L025-1	40°54′57″N, 123°10′5″E	Biotite schist	Gaojiayu Formation	2005–3331	LA-ICP-MS	Detrital zircon age	Luo et al. (2008)
47	04L046-4	40°23′37″N, 122°55′35″E	Fine-grained biotite gneiss	Gaojiayu Formation		LA-ICP-MS	Detrital zircon age	Luo et al. (2008)

Table 1 continued

No.	Samples	Location (GPS)	Lithologies	Formations/ intrusions	Ages (Ma)	Methods	Interpretations	References
48	02L098-1	40°51.763′N, 122°55.851′E	Graphite-bearing mica schist	Dashiqiao Formation	2012–2538	LA-ICP-MS	Detrital zircon age	Luo et al. (2004)
49	02L102-5	40°26.385′N, 122°48.584′E	Staurolite mica schist	Dashiqiao Formation		LA-ICP-MS	Detrital zircon age	Luo et al. (2004)
50	02L102-6	40°26.385′N, 122°48.584′E	Staurolite mica schist	Dashiqiao Formation		LA-ICP-MS	Detrital zircon age	Luo et al. (2004)
51	04L053-2	40°26.385′N, 122°48.584′E	Felsic gneiss	Dashiqiao Formation		LA-ICP-MS	Detrital zircon age	Luo et al. (2004)
52	LC3	40°51′40″N, 123°54′27″E	Muscovite schist	Gaixian Formation	1981–3520	LA-ICP-MS	Detrital zircon age	Li et al. (2015a)
53	LC5	40°51′40″N, 123°54′27″E	Meta-sandstone	Gaixian Formation		LA-ICP-MS	Detrital zircon age	Li et al. (2015a)
54	LB3	40°28′23″N, 123°52′42″E	Sericite phyllite	Gaixian Formation		LA-ICP-MS	Detrital zircon age	Li et al. (2015a)
55	04L031-3	40°33.062′N, 122°34.410′E	Fine-grained biotite gneiss	Gaixian Formation		LA-ICP-MS	Detrital zircon age	Luo et al. (2008)
56	DD07-5	40°43′47″N, 125°09′41″E	Granite gneiss	Gaixian Formation		LA-ICP-MS	Detrital zircon age	Meng et al. (2013a, b)
57	DD07-4	40°43′47″N, 125°09′41″E	Biotite-quartz schist	Gaixian Formation		LA-ICP-MS	Detrital zircon age	Meng et al. (2013a, b)
58	HY07-2	40°43′47″N, 125°09′41″E	Tourmaline-bearing leucoleptite	Gaixian Formation		LA-ICP-MS	Detrital zircon age	Meng et al. (2013a, b)
ca. 1.9 Ga metamorphism event								
59	Y1	Liaoning Province	Mica schist	Gaixian Formation	1896 ± 7	Ar–Ar	Metamorphic age	Yin and Nie (1996)
60	02L095-1	40°51.763′N, 122°55.849′E	Plagioclase-quartz schist	Langzishan Formation	1929 ± 38 ($n = 6$)	LA-ICP-MS	Metamorphic age	Luo et al. (2004)
61	04L053-2	40°26.385′N, 122°48.584′E	Felsic gneiss	Dashiqiao Formation	1930 ± 34 ($n = 8$)	LA-ICP-MS	Metamorphic age	Luo et al. (2004)
62	FW10-327	40°31′28″N, 122°47′54″E	Tourmaline muscovite granite	Hupiyu Pluton	1863 ± 37 ($n = 1$)	LA-ICP-MS	Metamorphic age	Lu et al. (2004a)
63	Lu0007	41°24′18″N, 125°36′37″E	Syenogranite	Qianzhuogou Pluton	1936 ± 10 ($n = 1$)	SHRIMP	Metamorphic age	Lu et al. (2004a)
64	LJ056	Mafeng Town, Haicheng City	Magnetite monzogranitic gneiss	Mafeng Pluton	1914 ± 13 ($n = 7$)	SHRIMP	Metamorphic age	Li and Zhao (2007)
65	04L023-1	40°55.102′N, 123°10.769′E	Banded biotite plagioclase gneiss	Lieryu Formation	1943 ± 55 ($n = 4$)	LA-ICP-MS	Metamorphic age	Luo et al. (2008)
66	04L045-1	40°23′41″N, 122°55′35″E	Fine-grained biotite gneiss	Lieryu Formation	1948 + 38/−31 ($n = 4$)	LA-ICP-MS	Metamorphic age	Luo et al. (2008)
67	03JH073	40°34′19″N, 122°35′23″E	Garnet-staurolite-mica schist	Gaixian Formation	1935–1914	PbSL	Metamorphic age	Xie et al. (2011)
68	N13	Houxianyu boron deposit	Hyalotourmalite	Lieryu Formation	1906 ± 4 ($n = 16$)	SHRIMP	Metamorphic age	Liu et al. (2012)
69	N02	Houxianyu boron deposit	Hyalotourmalite	Lieryu Formation	1889 ± 62 ($n = 4$)	SHRIMP	Metamorphic age	Liu et al. (2012)
70	DD07-5	40°43′47″N, 125°09′41″E	Granite gneiss	Gaixian Formation	1889 ± 12 ($n = 12$)	LA-ICP-MS	Metamorphic age	Meng et al. (2013a, b)
71	DD07-4	40°43′47″N, 125°09′41″E	Biotite-quartz schist	Gaixian Formation	1884 ± 12 ($n = 9$)	LA-ICP-MS	Metamorphic age	Meng et al. (2013a, b)

Table 1 continued

No.	Samples	Location (GPS)	Lithologies	Formations/ intrusions	Ages (Ma)	Methods	Interpretations	References
72	HY07-2	40°43′47″N, 125°09′41″E	Tourmaline-bearing leucoleptite	Gaixian Formation	1884 ± 18 ($n = 3$)	LA-ICP-MS	Metamorphic age	Meng et al. (2013a, b)
73	DZ78-1	Yanggoumen Country	Amphibolite	Dashiqiao Formation	1896 ± 22 ($n = 18$)	LA-ICP-MS	Metamorphic age	Meng et al. (2014)
74	DZ85-1	Tianshui Town	Meta-gabbro	Intrusion	1899 ± 26 ($n = 13$)	LA-ICP-MS	Metamorphic age	Meng et al. (2014)
75	DZ73-1	Daxingtun Country	Meta-gabbro	Intrusion	1900 ± 17 ($n = 5$)	LA-ICP-MS	Metamorphic age	Meng et al. (2014)
76	LZ08-1	40°32′24″N, 122°43′45″E	Amphibolite	Lieryu Formation	1895 ± 16 ($n = 41$)	LA-ICP-MS	Metamorphic age	Li and Chen (2014)
77	LZ04-1	40°32′24″N, 122°43′45″E	Fine-grained gneiss	Lieryu Formation	1919 ± 13 ($n = 1$)	LA-ICP-MS	Metamorphic age	Li and Chen (2014)
78	LZ12-1	40°32′24″N, 122°43′45″E	Amphibolite	Lieryu Formation	1876 ± 12 ($n = 21$)	LA-ICP-MS	Metamorphic age	Li et al. (2015a)
79	LZ03-1	40°32′24″N, 122°43′45″E	Mica schist	Lieryu Formation	1905 ± 8 ($n = 23$)	LA-ICP-MS	Metamorphic age	Li et al. (2015b)
1.82–1.87 Ga post-tectonic magmatism event								
80	12,082	41°11′14″N, 125°51′40″E	Rapakivi granite	Shuangcha Pluton	1817 ± 18 ($n = 5$)	SHRIMP	Crystallization age	Lu et al. (2004a, 2006) and Yang et al. (2015b)
81	12,082	41°11′14″N, 125°51′40″E	Rapakivi granite	Shuangcha Pluton	1769 ± 92 ($n = 5$)	TIMS	Crystallization age	Lu et al. (2004a, 2006)
82	92,015	41°14′3″N, 125°52′21″E	Porphyric granite	Shuangcha Pluton	1861 ± 9 ($n = 4$)	TIMS	Crystallization age	Lu et al. (2004a, 2006)
83	92,015	41°14′3″N, 125°52′21″E	Porphyric granite	Shuangcha Pluton	1872 ± 8 ($n = 14$)	SHRIMP	Crystallization age	Lu et al. (2004a, 2006)
84	Lu010-1	41°06′19″N, 125°06′49″E	Porphyric granite	Lujiabaozi Pluton	1773 ± 59 ($n = 5$)	TIMS	Crystallization age	Lu et al. (2004a, 2006)
85	Lu010-1	41°06′19″N, 125°06′49″E	Porphyric granite	Lujiabaozi Pluton	1841 ± 12 ($n = 5$)	SHRIMP	Crystallization age	Lu et al. (2004a, 2006)
86	12,072	41°28′24″N, 125°52′54″E	Quartz diorite	Qinghe Pluton	1872 ± 11 ($n = 12$)	SHRIMP	Crystallization age	Lu et al. (2004a, 2006)
87	FW02-62	40°19′21″N, 122°47′57″E	Porphyric granite	Wolongquan Pluton	1848 ± 10 ($n = 22$)	LA-ICP-MS	Crystallization age	Lu et al. (2004a)
88	FW01-31	40°10′04″N, 122°39′28″E	Hornblende pyroxene syenite	Kuangdonggou Pluton	1843 ± 23 ($n = 20$)	LA-ICP-MS	Crystallization age	Lu et al. (2004a)
89	03JH079	Gaixian area	Coarse-gained syenite	Kuangdonggou Pluton	1879 ± 17 ($n = 19$)	LA-ICP-MS	Crystallization age	Yang et al. (2007)
90	03JH080	Gaixian area	Fine-grained syenite	Kuangdonggou Pluton	1874 ± 18 ($n = 17$)	LA-ICP-MS	Crystallization age	Yang et al. (2007)
91	03JH082	Gaixian area	Fine-grained diorite	Kuangdonggou Pluton	1870 ± 18 ($n = 12$)	LA-ICP-MS	Crystallization age	Yang et al. (2007)
92	10JL13	40°51′59″N, 123°24′43″E	Granite pegmatite	Honghuagoumen Dyke	1870 ± 8 ($n = 13$)	LA-ICP-MS	Crystallization age	Wang et al. (2011a, b)
93	FX12-25/1	40°56′11″N, 122°47′14″E	Meta-gabbro	Intrusion	1816 ± 7 ($n = 16$)	CAMECA	Crystallization age	Yuan et al. (2015)

SHRIMP sensitive high-resolution ion microprobe, *CAMECA* Cameca ion microprobe, *LA-ICP-MS* laser ablation-inductively coupled plasma-mass spectrometry, *Ar–Ar* ^{40}Ar/^{39}Ar age, *SGDZ* single grain dissolution zircon U–Pb age, *Sm–Nd* Sm–Nd whole-rock/mineral isochron age

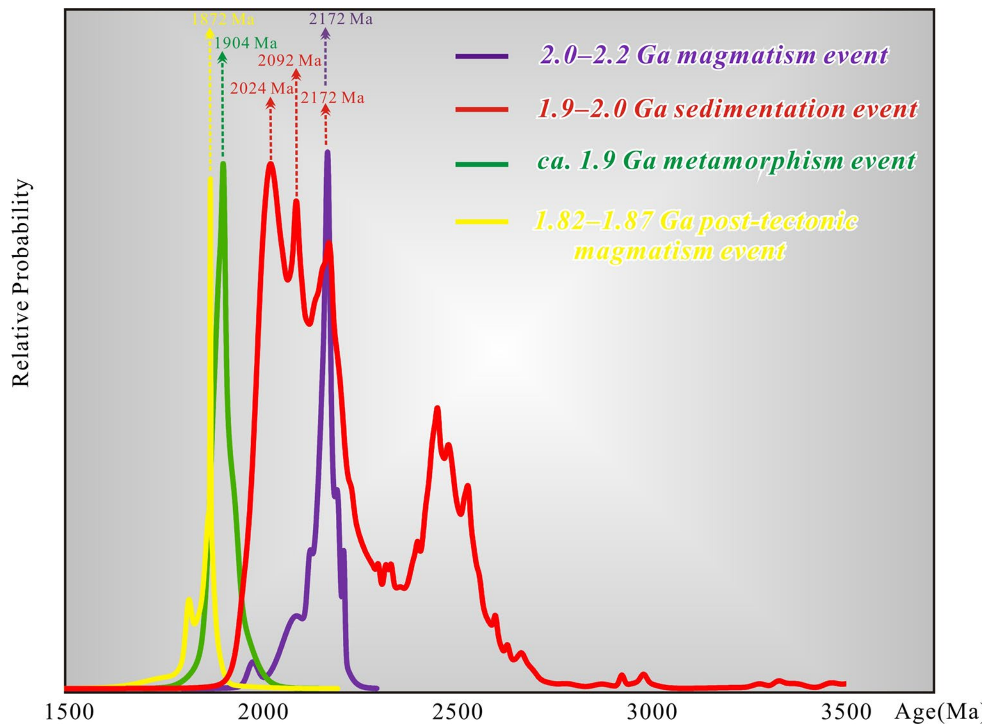

Fig. 3 Probability plot of the zircon U–Pb ages of the Paleoproterozoic rocks in the Liaodong Peninsula and adjacent regions (according to Table 1 and references therein)

graphite-bearing garnet–staurolite mica schists and kyanite-bearing mica schists. The conformably overlying Lieryu and Gaojiayu Formations occur in both the North and South Liaohe Groups and comprise boron-bearing volcano-sedimentary successions metamorphosed to fine-grained felsic gneisses, amphibolites and mica quartz schists. Overlying the Gaojiayu Formation is the Dashiqiao Formation that is present in both groups and is composed dominantly of dolomitic marbles intercalated with minor carbonaceous slates and mica schist. The uppermost Gaixian Formation is shared by both groups and consists of phyllites, andalusite–cordierite mica schists, staurolite mica schists and sillimanite mica schists, with minor quartzite and marbles (LBGMR 1989). The youngest igneous zircons identified from the analyzed meta-sedimentary rocks yield ages of 2.027 Ga (Langzishan Formation, Luo et al. 2004), 2.005 Ga (Lieryu and Gaojiayu Formations, Luo et al. 2008), 2.012 Ga (Dashiqiao Formation, Luo et al. 2008) and 1.981 Ga (Gaixian Formation, Li et al. 2015a, b; Meng et al. 2013a), which can constrain the maximum depositional age of the Liaohe Group. The minimum ages of the detrital zircons from the meta-sedimentary rocks indicate that the deposition age of the Liaohe Group is younger than 1981 ± 13 Ma (thus ca. 1980 Ma). Since the protoliths of the meta-sedimentary rocks should be deposited before the regional tectonic–metamorphic event at ca. 1.9 Ga (see next section for details), the depositional age of the Liaohe Group was 1.90–1.98 Ga (Fig. 3).

Metamorphism event (ca. 1.9 Ga)

The ca. 1.9 Ga regional tectonic–metamorphic event is well constrained by the evidence below: (a) the $^{40}Ar/^{39}Ar$ age of 1896 ± 7 Ma for biotites from a main detachment shear zone in the Liaohe Group (Yin and Nie 1996), (b) the concordant U–Pb age of ca. 1.9 Ga for the metamorphic overgrowth of zircons from the meta-sedimentary rocks (LA-ICP-MS method; Li et al. 2015b; Luo et al. 2004, 2008), (c) the age 1914 ± 13 Ma for the metamorphic overgrowth of zircons from the Liaoji granites using the SHRIMP technique (Li and Zhao 2007) and (d) $^{207}Pb/^{206}Pb$ metamorphic ages of 1.91–1.93 Ga for metamorphic phases such as garnet and staurolite from the meta-sedimentary rocks using the $^{207}Pb/^{206}Pb$ stepwise-leaching method (Xie et al. 2011). More recently, Meng et al. (2014) and Li and Chen (2014) obtained a concordant U–Pb age of ca. 1.9 Ga for the metamorphic zircons from the meta-mafic rocks, which were interpreted as the age of peak metamorphism of the Liaohe Group during collisional processes (Fig. 3).

Post-tectonic magmatism event (1.82–1.87 Ga)

The undeformed granite–syenite–pegmatite–mafic dykes crosscut the aforementioned metamorphosed volcano-sedimentary rocks in the Liaohe Group and foliated granite–mafic intrusions (Bai 1993; Zhang and Yang 1988). The emplacement of these post-tectonic magmas was determined using the zircon U–Pb method at 1.82–1.87 Ga (Li and Zhao 2007; Lu et al. 2004a, 2006; Wang et al. 2011a, b; Yang et al. 2007; Yuan et al. 2015), marking the end of the Paleoproterozoic tectonothermal event (Table 1; Fig. 3).

Discussion and conclusions

Can the Paleoproterozoic JLJB be a rift?

As mentioned above, the tectonic setting of the JLJB during the Mid-Paleoproterozoic between 2.2 and 1.8 Ga is still unclear. There are two opposite views on this issue: extension-dominant rifting regime and subduction–arc regime. Summarizing the characteristics of the Paleoproterozoic magmatism, sedimentation, metamorphism and metallogeny in the Liaodong Peninsula, we support the continental arc setting, based on the following reasons.

Evidence from the 2.0- to 2.2-Ga magmatism

1. A main argument for the rift model is the presence of bimodal volcanic rocks in the form of meta-basalts (greenschists and amphibolites) and meta-rhyolites (fine-grained gneisses; Peng and Palmer 1995, 2002; Sun et al. 1993, 1996; Zhang and Yang 1988). To verify it, we collected the geochemical compositions of volcano-sedimentary rocks in the study area. The volcano-sedimentary rocks have undergone greenschist- to amphibolite-facies metamorphism and deformation. It is therefore important to evaluate the effects of the metamorphism on the geochemistry before considering any petrogenetic interpretation. The studied rocks have not undergone significant secondary alteration as inferred from their low LOI of 0.5–4 % (most samples with loss of ignition <3 %), absence of Ce anomalies and lack of carbonization or silicification. Ague (1991) denoted that despite metamorphic grade up to amphibolite facies, mean weight percent of CaO, Na_2O and K_2O of volcano-sedimentary rocks remains essentially unchanged. Therefore, the major element data of the samples are convincing due to their low degree of mobility during metamorphism. Then we analyzed them on the protolith discrimination diagram (Simonen 1953) and selected only igneous rocks (samples in the shaded area of Fig. 4a) for further discussion. These igneous rocks define a single magmatic trend on the TAS and K_2O versus SiO_2 diagrams (Fig. 4b, c; Irvine and Baragar 1971; Middlemost 1994; Peccerillo and Taylor 1976), with the majority classified as subalkaline and no evidence of a bimodal distribution (Fig. 4b, c). In addition, it should be highlighted that our recent studies on the fine-grained gneisses (meta-felsic volcanic rocks) in the Liaodong Peninsula suggest that some of the volcanic rocks have andesitic composition, with mineralogy of hornblende/pyroxene (15–35 %), plagioclase (45–35 %), K-feldspar (~10–25 %) and quartz (~10 %) and SiO_2 in the range from 55 to 62 % (Fig. 5a–c; Li and Chen 2014; Chen et al. 2016 and our unpublished data). This is supported by the wide range of SiO_2 (54–75 %) reported for the fine-grained gneisses of the Liaohe Group (Zhang 1994).
2. The 2.0- to 2.2-Ga mafic rocks in the Liaodong Peninsula also provide important insights into the tectonic nature of the JLJB (Table 1). These rocks have chondrite-normalized REE patterns that are light REE enriched and have weakly negative to positive Eu anomalies (Faure et al. 2004; Li and Chen 2014; Meng et al. 2014; Wang et al. 2011a, b). Primitive-mantle-normalized multielement variation diagrams for these rocks are enriched in the large ion lithosphere elements (LILEs; e.g., Rb, Sr and Ba) and depleted in the high field strength elements (HFSEs; e.g., Nb, Ta, Zr and Hf), and the rocks have positive Pb and negative Ti anomalies, all of which are indicative of magmas that were formed in an arc-type setting (e.g., Meng et al. 2014). These rocks also have pronounced negative Nb, Ta and Ti anomalies, in contrast to typical plume-related or asthenosphere-derived magmas with trace-element patterns of OIB or MORB (Dong et al. 2012; Faure et al. 2004; Li and Chen 2014; Meng et al. 2014; Sun et al. 1993, 1996; Wang et al. 2011a, b; Yuan et al. 2015). In addition, the fact that these mafic rocks have arc-like geochemical compositions suggests that the mantle of these rocks was metasomatized by fluids and/or melts (Li and Chen 2014; Meng et al. 2014). There are no basaltic rocks with typical OIB-type compositions in this area, although such OIB-type basalts often generated in a continental rift environment (e.g., Furman 2007; Wilson 1989), meaning that the existing intracontinental rift model for this region is inconsistent with the arc-type affinities of the Paleoproterozoic rocks in this area. In addition, the 2.0 to 2.2 Ga mafic rocks have both tholeiitic and calc-alkaline affinities on discrimination diagrams (Fig. 4c–f; Cabanis and Lecolle 1989; Miyashiro 1975; Mullen 1983; Peccerillo and Taylor 1976), a feature that is again consistent with an arc-type setting. The mafic rocks in this area also provide ideal constraints on the subduction polarity. Faure et al. (2004) and Lu et al. (2006) suggested that the formation of the JLJB was related to south-directed subduction beneath the Nangrim Block, as evidenced by the southern location of the magmatic belt and the clockwise P–T path of the North Liaohe

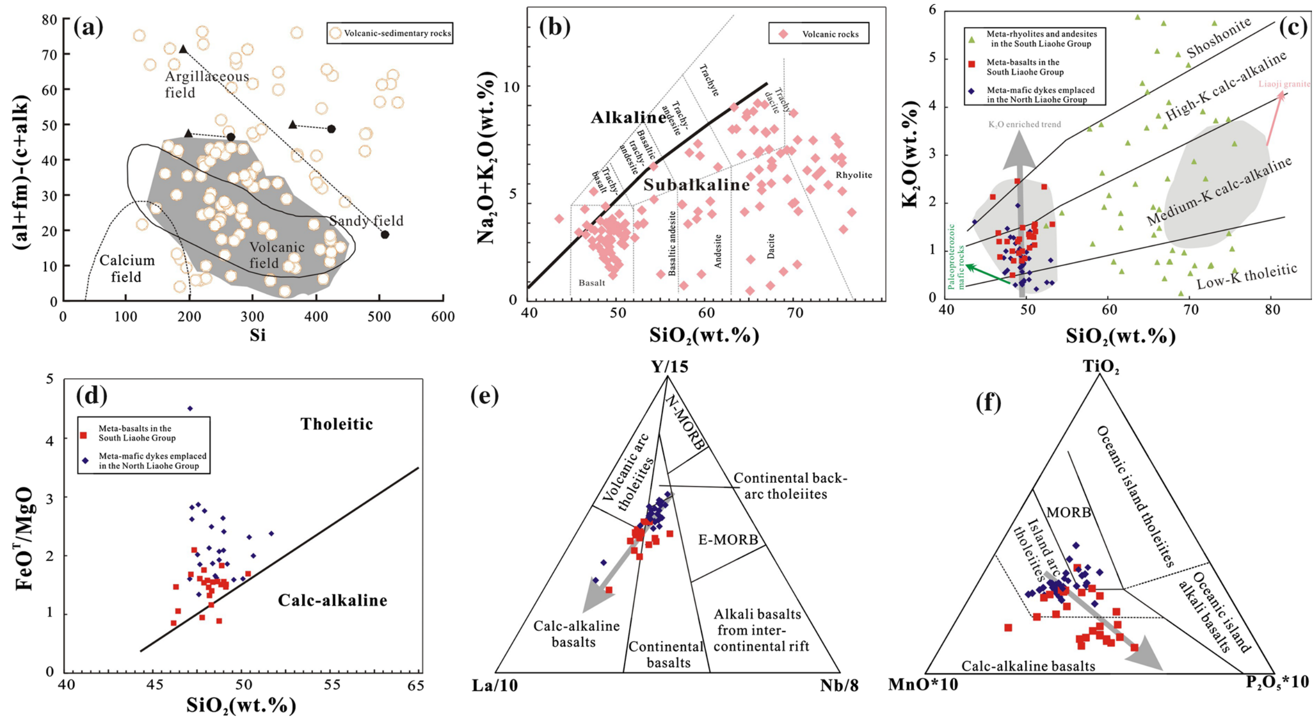

Fig. 4 A group diagrams of the petrogenesis discrimination for the Paleoproterozoic igneous rocks in the Liaodong Peninsula and adjacent regions. **a** Simonen diagram for the volcano-sedimentary successions, modified after Simonen (1953); **b** TAS diagram (modified after Irvine and Baragar 1977; Middlemost 1994), showing a consecutive subalkaline magma series; **c** K_2O versus SiO_2 diagram for the volcanic rocks and Liaoji granite–mafic intrusions (modified after Peccerillo and Taylor 1976); **d** FeO^T/MgO versus SiO_2 diagram after Miyashiro1975; **e** La/10–Y/15–Nb/8 diagram after Cabanis and Lecolle (1989) and **f** TiO_2–MnO–P_2O_5 diagram after Mullen (1983), emphasizing tholeiite to calc-alkaline series in the north and the calc-alkaline in the south. *Data sources* volcanic-sedimentary rocks (Zhang and Yang 1988; Zhang 1994), meta-rhyolites and andesites in the South Liaohe Group (Zhang and Yang 1988; Zhang 1994; Sun et al. 1993, 1996; Chen et al. 2016), meta-basalts in the South Liaohe Group (Li and Chen 2014; Sun et al. 1993, 1996; Meng et al. 2014) and meta-mafic dykes emplaced in the North Liaohe Group (Meng et al. 2014; Wang et al. 2011a, b; Yuan et al. 2015)

Group, which need evidence supported this hypothesis. Figure 4c shows that mafic rocks within the North Liaohe Group and South Liaohe Group have tholeiitic to calc-alkaline and calc-alkaline compositions, respectively, consistent with their trace and major element compositions (Fig. 4d–f). The concentration of K_2O (at equivalent SiO_2 concentration) in basaltic rock increases with increasing distance from ocean to continent, as tholeiitic magmas generally occur near the trench and the calc-alkaline magmas near the continent in a single subduction system (Wilson 1989). This indicates that the distribution of the Paleoproterozoic mafic rocks in the study area, with tholeiitic to calc-alkaline rocks in the north and calc-alkaline rocks in the south, also provides evidence of south-directed subduction.

3. Finally, the Paleoproterozoic Liaoji granites (known as gneissic granites in this area; 2.1–2.2 Ga; Table 1) are also calc-alkaline (Hao et al. 2004; Lu 2004; Lu et al. 2004a, b) rather than A-type granites as was previously suggested (Fig. 4c). The previously identified A-type granites can be classified to two types: One is the A-type granites formed at 1.82–1.87 Ga (e.g., Shuangcha rapakivi granite and Kuangdonggou syenite; Table 1) or Mesozoic (e.g., Dandong and Gaoliduntai granites); the other is the highly fractionated I-type granites formed at 2.1–2.2 Ga. For example, Li et al. (2004) reported SHRIMP U–Pb zircon ages of 157 and 156 Ma for the Dandong and Gaoliduntai granites, respectively. Yang et al. (2007) reported LA-ICP-MS U–Pb zircon ages of 1870–1879 Ma for the Kuangdonggou syenites and diorites. Yang et al. (2015b) reported LA-ICP-MS U–Pb zircon ages of 1895 Ma for the Shuangcha megaporphyritic granites in the southern Jilin Province. These have long been considered to be Paleoproterozoic in age, but their reliable isotopic ages indicated not. Indeed, some granites (e.g., the Dafangshen pluton, high SiO_2 contents = 76.7–77.1 wt%) were formed at ca. 2.18 Ga and show A-type granite characteristics. However, it should be noted that tourmaline is a common accessory minerals in the plutons. Lukkari and Holtz (2007) proposed that addition of boron

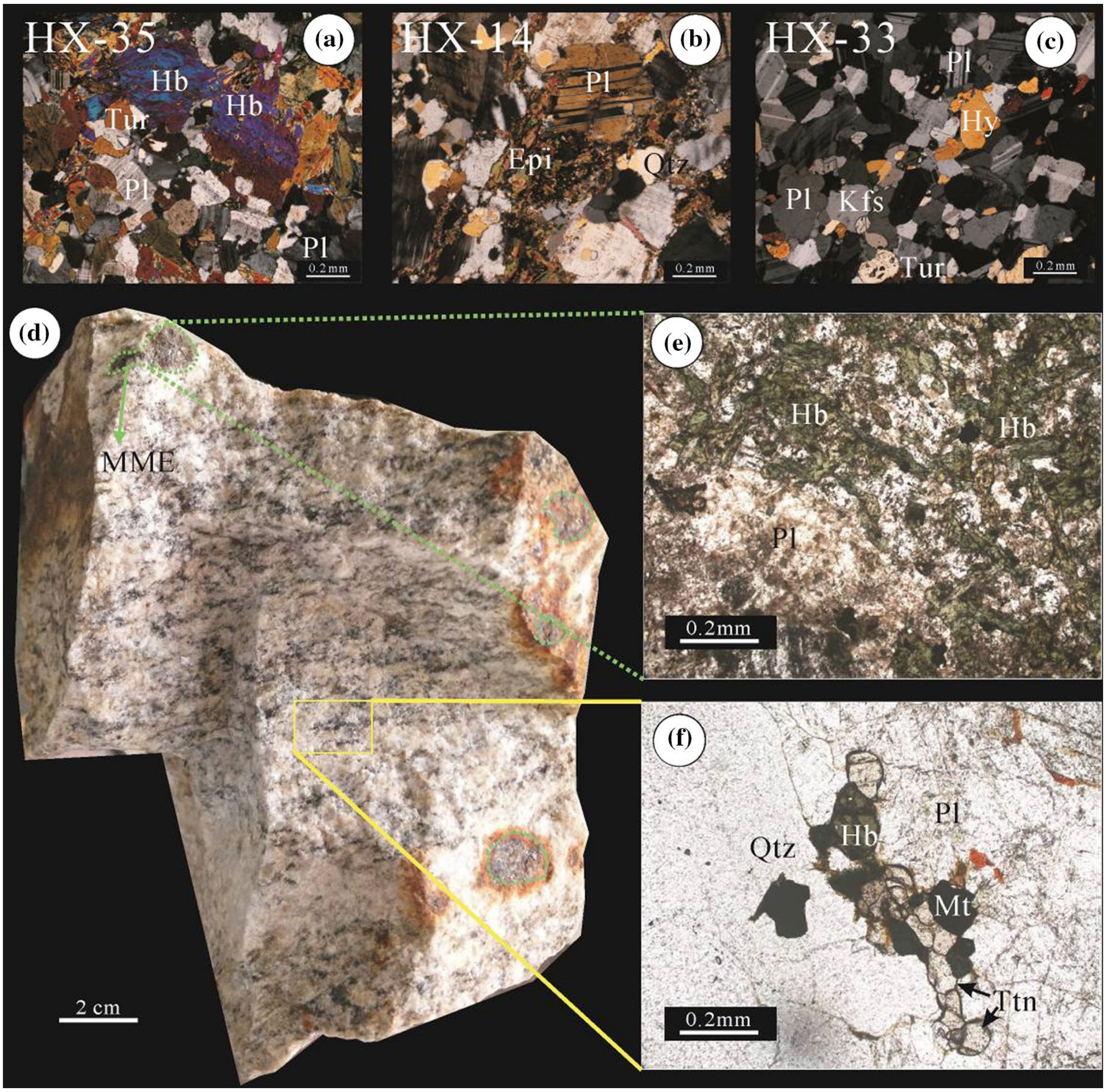

Fig. 5 Photographs of the respective rocks in the Liaodong Peninsula. *a–c* Photomicrographs of the volcanic rocks of andesitic composition, with mineralogy of hornblende/pyroxene (15–35 %), plagioclase (45–35 %), K-feldspar (~10–25 %) and quartz (~10 %) and SiO_2 in the range from 55 to 62 %; *d* A photograph of the representative Liaoji granite with mafic microgranular enclaves (MMEs). *e* A photomicrograph of the representative MMEs. *f* A photomicrograph of the Liaoji granite. Note the common occurrence of the MMEs (in the *green circle* in Fig. 4d), hornblende, magnetite and sphene within the host rock (Fig. 4d, e). *Pl* plagioclase, *Q* quartz, *Hb* hornblende, *Mt* magnetite, *Ttn* titanite, *Tur* tourmaline, *Epi* epidote, *Hy* hypersthene

in magma system tends to prolong magma evolution and leads to significant differentiation. Thus, the A-type-like characteristics are likely attributable to the highly evolved nature of the plutons (Yang et al. 2015a). Conspicuously, the majority of the Paleoproterozoic Liaoji granites could be basically water-enriched I-type granites (Fig. 4c), as shown by (a) the common occurrences of hornblendes, titanites, magnetites and MMEs (Fig. 5d–f; Chen et al. 2016; Li et al. 2015b; Yang et al. 2015a), suggesting a calc-alkaline, H_2O-rich and high fO_2 affinity of the parental magma, typical of I-type granites; (b) enriched in LILEs (such as K, Rb, Sr and Cs) and depleted in some HFSEs (such as Nb, Ta and Th), while A-type granites are generally enriched in the HFSEs (Whalen et al. 1987); (c) different from those of A-type granites which are always characterized by significant negative Eu anomalies and tetrad effects; and (d) large variation of whole-rock $\varepsilon_{Nd}(t)$ values (−8.6 to +1.5) and zircon $\varepsilon_{Hf}(t)$ values (−1.3 to +5.6), suggesting that mixing/mingling of lower crust-derived felsic magma with enriched mantle-derived mafic magma might have resulted in formation of these gneissic granites (Li et al. 2015b; Yang et al. 2015a). This means that the voluminous Paleoproterozoic A-type granites described previously, another line of evidence used to support a rift model, are also questionable.

Evidence from the 1.9- to 2.0-Ga sedimentation

A $^{207}Pb/^{206}Pb$ age spectrum of total 1042 detrital zircon analyses obtained from the Liaohe Group (and its equivalents) and is shown in Fig. 3. The three major peaks at 2024, 2092 and 2174 Ma shown in the age spectrum are well consistent with the age of meta-volcanic rocks of the Liaohe Group and Paleoproterozoic gneissic granite–mafic intrusions as mentioned. Furthermore, minor amounts of detrital zircons from the Liaohe Group yield ages between 2.45 and 3.52 Ga. These older detrital zircons of Archean age must have been transported from the two adjacent Archean blocks (Li et al. 2015a, b; Luo et al. 2004, 2008; Meng et al. 2014). Cawood et al. (2012) first established that detrital zircon spectra have distinctive age distribution patterns that reflect the tectonic setting of the basin in which they are deposited. Conspicuously, they proposed that there are significant differences between settings in the proportion of zircon ages associated with the youngest and much older magmatic events. Convergent margin basins have a high proportion of detrital zircons (generally >50 %) with ages close to the age of the sediment, and collisional basin generally contains a significant proportion of grains (10–50 %) with ages within 150 Ma of the host sediment, while extensional basins are dominated by detrital zircon ages that are much older than the time of sediment accumulation with <5 % of grains having ages within 150 Ma of the depositional age. As mentioned before, the depositional age of Liaohe Group should be 1.98–1.90 Ga and we adopt depositional age 1.94 Ga to discuss the characteristics of the provenance. It is worth to note that the zircons with age of 1.94–2.29 Ga constitute the largest proportion (~70 %) in the detrital zircon spectra, while the Archean zircons only occupy ~20 %, remarkably similar to those of back-arc or fore-arc basins in the North America Craton (Cawood et al. 2012; Condie et al. 1992). By plotting the distribution of the difference between the measured crystallization ages of individual zircon grains present in the sediment and the depositional age of the sediment, we can easily find that curve of the Liaohe Group falls in the convergent or collisional basin setting, entirely different from the rift basin. However, we are not able to unequivocally distinguish whether it were formed at the convergent basin or collisional basin setting, because these two settings are misty in the boundary solely based on detrital zircon ages (Fig. 6). Thus, the age patterns of detrital zircons suggest that the Paleoproterozoic arc-related rocks

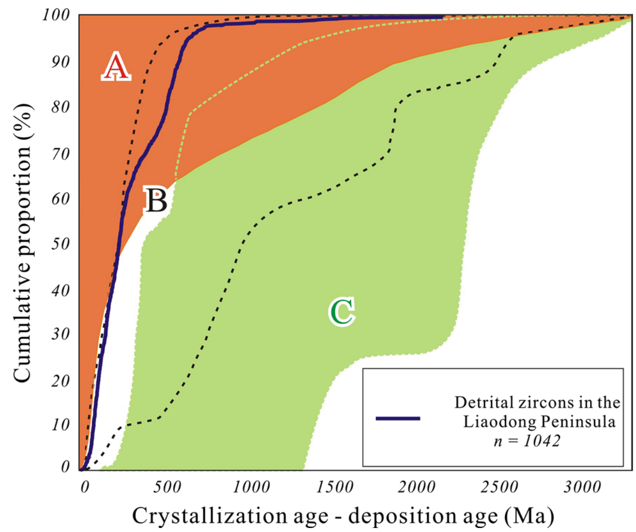

Fig. 6 Plot of detrital zircons in the Liaodong Peninsula ($n = 1042$). Note deposition age 1.94 Ga for the Paleoproterozoic meta-sedimentary rocks. The general fields for convergent (*A*: *orange* field), collisional (*B*: *black dashed line circled* field) and extensional basins (*C*: *green* field) are after Cawood et al. (2012) and references therein

(meta-volcanic rocks of the Liaohe Group and Paleoproterozoic Liaoji granites) in the JLJB are the major source rocks, and the Archean basement of the Eastern Block is the subordinate provenance (Li et al. 2015a, b). Such a combination of major arc-related lithologies and minor craton-derived sources is also indicated by trace-element geochemistry and Nd isotopes of the meta-sediments from the Liaohe Group. On the tectonic discrimination plots, the Paleoproterozoic meta-sedimentary rocks from the Liaohe Group display arc-like geochemical affinities, falling into the fields of continental island arc and active continental margin (Fig. 7). Thus, these rocks were probably deposited in a back-arc or fore-arc basin within an active continental margin or a continental island arc setting at 1.90–1.98 Ga. The youngest zircon recognized in the Liaohe Group indicates no production of subduction-triggered magmatism after 1.98 Ga. That is, the Nangrim Block was proximal to the Longgang Block at 1.90–1.98 Ga and a marginal sea may exist between them. Taking into account the similar zircon U–Pb ages and Hf isotope data for the North and South Liaohe groups (Li et al. 2015a, b; Luo et al. 2004, 2008; Meng et al. 2013a), they might be deposited in the same basin, such as back-arc or fore-arc basin, or distinctive basins with the same provenance. The distribution and rock associations of the North and South Liaohe Groups provide important clues to settle this question. Lithologically, the North Liaohe Group is dominated by clastic sediments and carbonates, metamorphosed to the quartzites, schists, phyllites and marbles. Besides, the sedimentary cycle is obvious, with a transition from a lower arkose- and volcano-sedimentary sequence

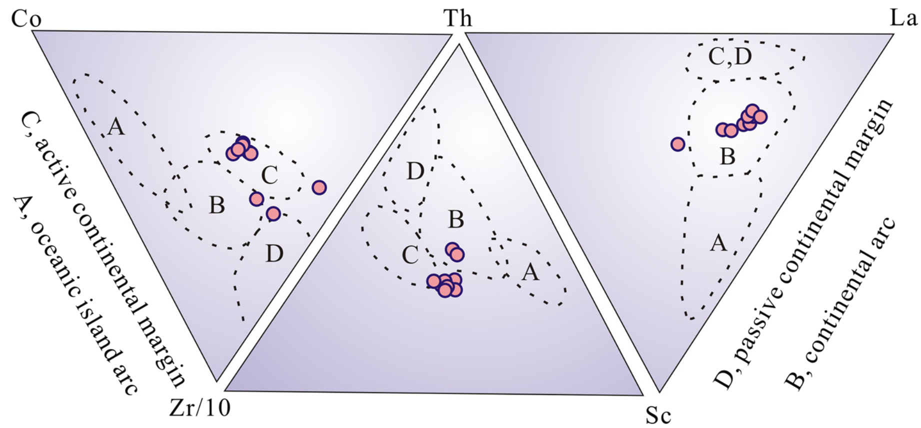

Fig. 7 Tectonic discrimination diagrams for the Paleoproterozoic metasedimentary rocks (modified after Li et al. 2015b)

(Langzishan, Lieryu and Gaojiayu Formations), through a middle carbonate-rich sequence (Dashiqiao Formation) to an upper argillaceous sequence (Gaixian Formation; Bai 1993; Lu et al. 2006; Sun et al. 1993, 1996). Considering that it is closed associated with fore-arc tholeiites (Chen et al. 2016; Meng et al. 2014; Yuan et al. 2015), we propose that the North Liaohe Group was deposited in a fore-arc basin. By contrast, the southern part of the JLJB, however, is dominated by the Paleoproterozoic volcanic rocks (the South Liaohe Group, with no obvious sedimentary cycle) and Paleoproterozoic Liaoji granites, probably formed in an arc setting (Bai 1993; Lu et al. 2006; Sun et al. 1993, 1996). The back-arc basin is the most likely deposit environment responsible for the South Liaohe Group.

Evidence from the ca. 1.9-Ga metamorphism

With the detailed field- and thermodynamics-based metamorphic investigations carried on the JLJB, significant differences have been recognized in metamorphism of the North and South Liaohe Groups, which show contrasting geological occurrences, mineral assemblages, physicochemical conditions of peak metamorphism and so on (He and Ye 1998; Li et al. 2005; Lu 1996; Lu et al. 2006; Zhao et al. 2005; Zhao and Zhai 2013). Garnet, staurolite and kyanite are common minerals in the North Liaohe Group. The North Liaohe Group is characterized by a clockwise P–T path, as evidenced by sillimanite replacing kyanite. Conspicuously, the metamorphism history can be reduced to a lower amphibolite-facies peak P–T stage followed by a subsequent isothermal decompression (ITD) process, consistent with the medium-pressure facies series (Fig. 8; He and Ye 1998; Zhao and Zhai 2013). Garnet, staurolite, andalusite, sillimanite and cordierite are common minerals in the South Liaohe Group. The South Liaohe Group is characterized by an anticlockwise P–T path, as evidenced by sillimanite replacing andalusite. Conspicuously, the metamorphic history can be reduced to a higher amphibolite-facies peak P–T stage followed by a subsequent isobaric cooling (IBC) process, consistent with the low-pressure facies series (Fig. 8; He and Ye 1998; Zhao and Zhai 2013). With respect to different rock associations and metamorphic histories, they are the same cases as Ji'an and Laoling Groups in southern Jilin and the Jingshan and Fenzishan Groups in eastern Shandong (Zhao et al. 2005; Zhao and Zhai 2013). Thus, the rift model cannot explain the different lithologies of the North and South Liaohe Groups, as well as the clockwise P–T paths and polyphase compressive deformation of the Laoling, North Liaohe and Fenzishan Groups (Li et al. 2012; Zhao and Zhai 2013). We proposed that the North and South Liaohe Groups were finally united together during the process of collision between the Longgang and Nangrim Blocks in the Late Paleoproterozoic (Li and Chen 2014; Li et al. 2015a, b, 2016a).

Evidence from the borate deposits

Recent studies have delineated that boron ore deposits are commonly present in the extensional basins formed in a convergent background (Floyd et al. 1998; Jiang et al. 1999), e.g., Loma Blanca borate deposit in Argentina (Alonso et al. 1988), which were probably derived from a boron-rich mantle source that had been previously metasomatized by subduction zone boron-rich fluids released from seawater-altered oceanic crust and/or pelagic sediments (Palmer 1991; Peng and Palmer 1995, 2002; Ryan and Langmuir 1993). However, due to the extremely low boron content of the lower continental crust and mantle, boron enrichment is uncommon in continental rifts (Peng and Palmer 2002). In the previous sections, we mentioned that the meta-volcanic rocks of the Liaohe Group, in particular those of the Lieryu Formation, are characterized by enrichment of boron (Wang et al. 2008), as is indicated by the occurrence of a couple of big borate deposits in the fine-grained gneisses (Jiang 1987; Jiang et al. 1997; Peng

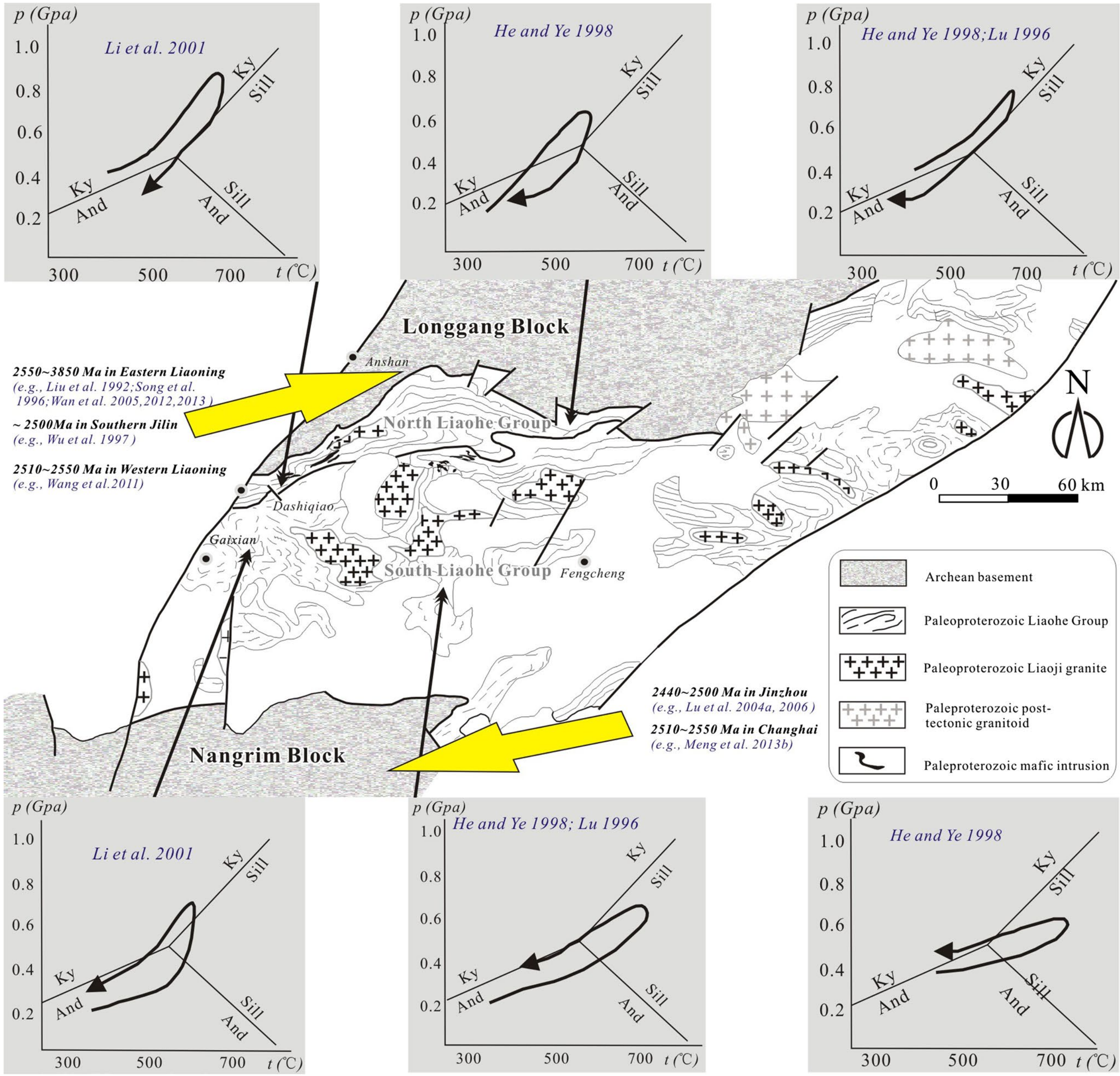

Fig. 8 P–T–t paths of the Liaohe Group (its equivalents) and ages of the Archean basement. Data sources: P–T–t paths (He and Ye 1998; Li et al. 2011; Lu 1996) and ages (Liu et al. 1992; Lu et al. 2004a, 2006; Meng et al. 2013b; Song et al. 1996; Wan et al. 2005, 2012, 2013; Wang et al. 2011a, b; Wu et al. 1997)

and Palmer 1995; Yan and Chen 2014). Tourmalines from the tourmaline-rich rocks (e.g., tourmalinite and tourmaline-rich quartz vein) show varied B isotope values ranging from +4.51 to +12.43 ‰. The B isotope value spectrum has a major peak at +8.67 ‰ (Fig. 9), which plot intermediate between those of the terrigenous sediments and arc rocks with low boron isotope values and marine evaporates with high boron isotope values. Non-marine evaporates (with $\delta^{11}B = -30.1$ to $+7$ ‰; Swihart et al. 1986) are unlikely to elevate the $\delta^{11}B$ values of borate minerals to so high levels. In addition, the Mg-rich carbonates and volcano-sedimentary rocks both share the high boron contents ($B_2O_3 = 3670$ ppm; Zhang 1994; $B_2O_3 = 500$–4000 ppm; Wang et al. 2008, respectively). Yan and Chen (2014) thus suggested that Paleoproterozoic metamorphic volcano-sedimentary rocks and the marine Mg-rich carbonates/silicates could be the principal boron sources for the Houxianyu borate deposit in the Liaodong Peninsula, strongly supported by the close spatial relationship between borate ore-body and the Mg-carbonates and Mg-silicates. Besides

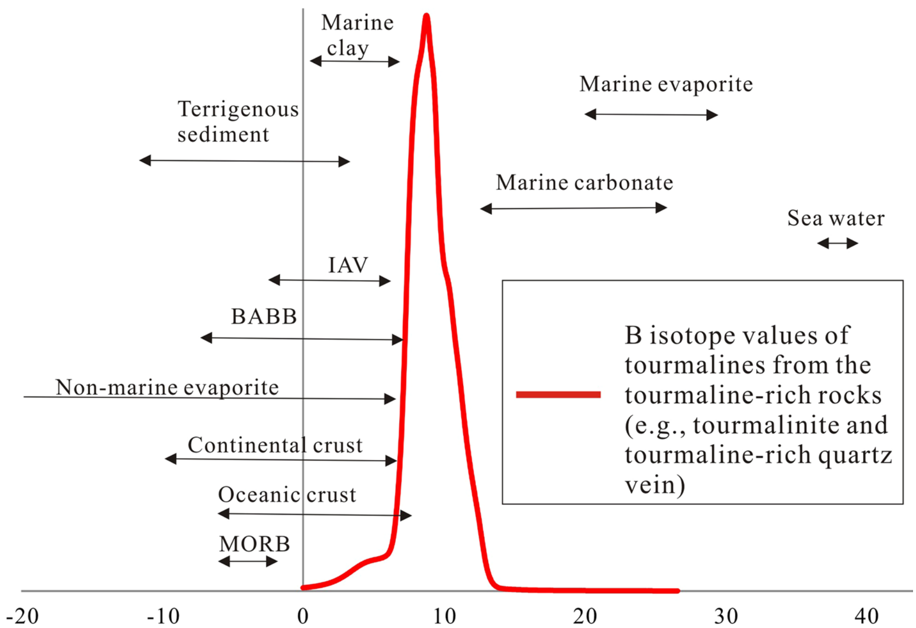

Fig. 9 Plot of boron isotopic compositions of tourmalines from the tourmaline-rich rocks (modified after Yan and Chen 2014; Peng and Palmer 2002; Jiang et al. 1997)

the B isotope value, other lines of evidence supported the marine environment of Mg-carbonates is described below. (a) The borate ore-bodies are associated with the Mg-carbonate, silicalite and stratiform tourmalinite in the Paleoproterozoic JLJB. Previous studies suggest that stratiform tourmalinite is commonly precipitated in a submarine environment as hydrothermal sedimentary rocks (Slack et al. 1993). This is consistent with the presence of anhydrite, an indication of marine environment (Peng and Palmer 1995). (b) Zhang (1994) carried out the O isotope study on the Paleoproterozoic rocks in the JLJB and revealed $\delta^{18}O = +10$ to $+21$ ‰ for the Mg-carbonate and borate phases. The average O isotope value of the marine carbonates is +14 ‰, suggesting a marine environment for the borate deposits and related Mg-carbonates. (c) The $\delta^{34}S$ values of pyrites from the borate ore-body range from +9.1 to +17.3 ‰ and those of pyrites from the host rocks in the range from +2.5 to +16.1 ‰ (Wang and Han 1989). The strong positive $\delta^{34}S$ values suggest a marine environment for pyrites, because marine evaporate sulfate commonly has $\delta^{34}S$ values ranging from +10 to +35 ‰ (Hölser 1977). The evidence above is inconsistent with the non-marine of an intracontinental rift, but supports a marine environment within an active continental margin or a continental island arc setting.

Evidence from the Archean basement

In addition, the arc affinity of the JLJB rocks is supported by geological data of the Archean basement. The Nangrim and Longgang Blocks show considerable differences in terms of lithological units, geochronology and metamorphic features. In the Nangrim Block, the Archean gneisses are dominated by quartz diorite and granodiorite (Fig. 10d) that were emplaced between 2540 and 2440 Ma and experienced amphibolite-facies metamorphism (Lin et al. 1992; Lu et al. 2004a, 2006; Meng et al. 2013b), whereas the Archean rocks in the Longgang Block are mainly TTG gneisses (charnockites and small amounts of supracrustal sequence; Fig. 10a–c) with much older protolith ages of 3850–2500 Ma (Figs. 9, 10; Liu et al. 1992; Jahn et al. 2008; Song et al. 1996; Wan et al. 2005, 2012, 2013; Wu et al. 1997) and amphibolite- to granulite-facies metamorphism (Lin et al. 1992; Liu et al. 1992; Song et al. 1996). The evidence can hardly support that two Archean blocks have been formed by splitting of a single craton; therefore, the rift model does not comply with our data. On the contrary, in the present state of knowledge, the arc-continent collision model appears as the most likely geodynamic interpretation of the JLJB.

Geodynamic scenario: a summary

We tentatively propose a new model (Fig. 11) to explain the genesis and geodynamic setting of Paleoproterozoic rocks in the Liaodong Peninsula.

1. In the period 2.0–2. 2 Ga, the Paleoproterozoic oceanic slab between the Nangrim and Longgang Blocks experienced a southward subduction beneath the Nangrim Block. This resulted in the formation of abundant arc rocks along the margin of the Nangrim Block, represented by the volcanic rocks of the Liaohe Group and coeval Liaoji granite–mafic intrusions (Fig. 11a).

Fig. 10 Photographs of the rocks from Archean Longgang and Nangrim Blocks. **a** TTG gneiss in the Longgang Block. **b** Charnockite in the Longgang Block. **c** BIF in the Longgang Block and **d** Quartz diorite–granodiorite in the Nangrim Block

Fig. 11 Cartoon showing tectonic evolution of the JLJB in the Paleoproterozoic. See text for details

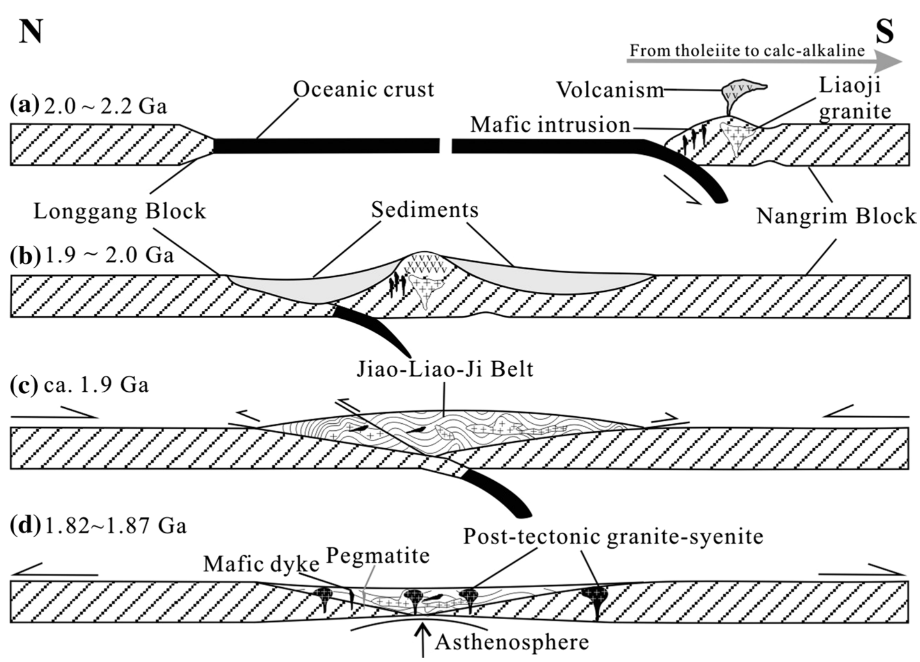

2. The sedimentary rocks of the Liaohe Group were deposited in the arc-related basin during the period 1.9–2.0 Ga (Fig. 11b).
3. The Liaohe Group and associated Liaoji granite–mafic intrusions were subsequently deformed and metamorphosed during the processes of arc-continent collision at ca. 1.9 Ga (Fig. 11c).
4. The undeformed granite–syenite–pegmatite–mafic dykes were emplaced in and crosscut the folded Paleoproterozoic metamorphosed volcano-sedimentary rocks and gneissic granite–mafic intrusions due to a process of post-collisional extension at 1.82–1.87 Ga (Fig. 11d).

Acknowledgments We thank Editor in Chief Prof. Wolf-Christian Dullo, Associate Editor Prof. Wenjiao Xiao and two reviewers (Dr. Hafiz Ur Rehman and an anonymous journal reviewer) for their constructive comments and careful corrections that led to significant improvement to the manuscript. We express our gratitude to Dr. Yan Zhan, Dr. Jiahui Qian, Dr. Chuan Yang, Dr. Jialin Wang, Dr. Jie Dong, Dr. Maohui Ge, Dr. Chao Li and Dr. Ting Liu for their discussions. This work was financially supported by the National Key Basic Research Program of China (Grant No. 2012CB416603), the National Natural Science Foundation of China (Grant No. 90914001), the Opening Foundation of the Peking University (Grant No. 0000010541) and the Undergraduates Innovating Experimentation Project of Jilin University (Grant No. 2010C61164).

References

Ague JJ (1991) Evidence for major mass transfer and volume strain during regional metamorphism of pelites. Geology 19:855–858

Alonso RN, Helvaci C, Sureda RJ, Viramonte JG (1988) A new Tertiary borax deposit in the Andes. Miner Depos 23:299–305

Bai J (1993) The precambrian geology and Pb–Zn mineralization in the northern Margin of North China Platform. Geological Publishing House, Beijing, pp 47–89 **(in Chinese with English abstract)**

Baines AG, Cheadle MJ, John BE, Grimes CB, Schwartz JJ, Wooden JL (2009) SHRIMP Pb–U zircon ages constrain gabbroic crustal accretion at Atlantis Bankon the ultraslow-spreading Southwest Indian Ridge. Earth Planet Sci Lett 287:540–550

Cabanis B, Lecolle M (1989) Le diagramme La/10–Y/15–Nb/8: Un outil pour la discrimination des series volcaniques et la mise en evidence des procesus de melange et/ou de contamination crutale. Comptes Rendus l'Acad Sci 309:2023–2029

Cawood PA, Hawkesworth CJ, Dhuime B (2012) Detrital zircon record and tectonic setting. Geology 40:875–878

Chen B, Li Z, Wang JL, Zhang L, Yan XL (2016) Liaodong Peninsula ~2.2 Ga magmatic event and its geological significance. J Jilin Univ (Earth Sci Edn) 461:303–320 **(in Chinese with English abstract)**

Condie KC, Noll PD, Conway CM (1992) Geochemical and detrital mode evidence for sources of early Proterozoic sedimentary-rocks from the Tonto Basin Supergroup, Central Arizona. Sed Geol 77:51–76

Dong CY, Ma MZ, Liu SJ, Xie HQ, Liu DY, Li XM, Wan YS (2012) Middle Paleoproterozoic crustal extensional regime in the North China Craton: new evidence from SHRIMP zircon U-Pb dating and whole-rock geochemistry of meta-gabbro in the Anshan-Gongchangling area. Acta Petrol Sin 28:2785–2792 **(in Chinese with English abstract)**

Faure M, Lin W, Monie P, Bruguier O (2004) Paleoproterozoic arc magmatism and collision in Liaodong Peninsula (north-east China). Terra Nova 16:75–80

Floyd PA, Helvaci C, Mittwede SK (1998) Geochemical discrimination of volcanic rocks associated with borate deposits: an exploration tool? J Geochem Explor 60:185–205

Furman T (2007) Geochemistry of East African Rift basalts: an overview. J Afr Earth Sci 48:147–160

Gao S, Rudnick RL, Yuan HL, Liu XM, Liu YS, Xu WL, Ling WL, Ayers J, Wang XC, Wang QH (2004) Recycling lower continental crust in the North China Craton. Nature 432:892–897

Hao DF, Li SZ, Zhao GC, Sun M, Han ZZ, Zhao GT (2004) Origin and its constraint to tectonic evolution of Paleoproterozoic granitoids in the eastern Liaoning and Jilin province, North China. Acta Petrol Sin 20:1409–1416 **(in Chinese with English abstract)**

He GP, Ye HW (1998) Two types of early Proterozoic metamorphism in the eastern Liaoning to southern Jilin and their tectonic implication. Acta Petrol Sin 14:152–162 **(in Chinese with English abstract)**

Hölser DJ (1977) Catastrophic chemical events in the history of the ocean. Nature 267:403–408

Irvine TH, Baragar WRA (1971) A guide to the chemical classification of the common volcanic rocks. Can J Earth Sci 8:523–548

Jahn BM, Liu D, Wan Y, Song B, Wu J (2008) Archean crustal evolution of the Jiaodong Peninsula, China, as revealed by zircon SHRIMP geochronology, elemental and Nd-isotope geochemistry. Am J Sci 308:232–269

Jiang CC (1987) Precambrian geology of eastern part of Liaoning and Jilin. Liaoning Science and Technology Publishing House, Shenyang

Jiang SY, Palmer MR, Peng QM, Yang JH (1997) Chemical and stable isotopic compositions of Proterozoic metamorphosed evaporites and associated tourmalines from the Houxianyu borate deposit, eastern Liaoning, China. Chem Geol 1997:189–211

Jiang SY, Palmer MR, Slack JF, Shaw DR (1999) Boron isotope systematics of tourmaline formation in the Sullivan Pb–Zn–Ag deposit, British Columbia, Canada. Chem Geol 158:131–144

Koglin N, Kostopoulos D, Reischmann T (2009) The Lesvos mafic–ultramafic complex, Greece: ophiolite or incipient rift? Lithos 108:243–261

LBGMR (Liaoning Bureau of Geology and Mineral Resources) (1989) Regional geology of Liaoning Province. Geological Publishing House, Beijing, pp 56–126 **(in Chinese with English abstract)**

Li Z, Chen B (2014) Geochronology and geochemistry of the Paleoproterozoic meta-basalts from the Jiao-Liao-Ji Belt, North China Craton: implications for petrogenesis and tectonic setting. Precambr Res 255:653–676

Li SZ, Zhao GC (2007) SHRIMP U–Pb zircon geochronology of the Liaoji granitoids: constraints on the evolution of the Paleoproterozoic Jiao-Liao-Ji Belt in the Eastern Block of the North China Craton. Precambr Res 158:1–16

Li HK, Li HM, Lu SN (1995) Grain zircon U–Pb age for volcanic rocks from Tuanshanzi formation of Changcheng system and their geological implication. Geochimica 24:43–48 **(in Chinese with English abstract)**

Li SZ, Han ZZ, Liu YJ, Yang ZS (2001) Constraints of geology and geochemistry on Palaeoproterozoic pre-orogenic deep processes in Jiao-Liao Massif. Sci Geol Sin 36:184–194 **(in Chinese with English abstract)**

Li SZ, Zhao GC, Sun M, Wu FY, Liu JZ, Hao DF, Han ZZ, Luo Y (2004) Mesozoic, not Paleoproterozoic SHRIMP U–Pb zircon ages of two Liaoji Gran-ites, Eastern Block, North China Craton. Int Geol Rev 46:162–176

Li SZ, Zhao GC, Sun M, Han ZZ, Luo Y, Hao D, Xia XP (2005) Deformation history of the Paleoproterozoic Liaohe assemblages in the Eastern Block of the North China Craton. J Asian Earth Sci 24:659–674

Li SZ, Zhao GC, Sun M, Han ZZ, Zhao GT, Hao DF (2006) Are the South and North Liaohe Groups of North China Craton different exotic terranes? Nd isotope constraints. Gondwana Res 9:198–208

Li SZ, Zhao GC, Santosh M, Liu X, Dai LM (2011) Palaeoproterozoic tectonothermal evolution and deep crustal processes in the Jiao-Liao-Ji Belt, North China Craton: a review. Geol J 46:525–543

Li SZ, Zhao GC, Santosh M, Liu X, Lai LM, Suo YH, Song MC, Wang PC (2012) Structural evolution of the Jiaobei Massif in the southern segment of the Jiao-Liao-Ji Belt, North China Craton. Precambr Res 200–203:59–73

Li Z, Pei FP, Meng E (2014a) Zircon U–Pb age, geochemical and Nd isotopic data of the Middle Jurassic high-Mg dioritic dike in the Liaodong Peninsula, NE China. Glob Geol 17:143–154

Li Z, Wang JL, Wang M, Zhang L, Liu JW, Qian JH, Yu HL (2014b) Redefinition of the Langzishan formation in the North Liaohe Group. Adv Geosci 4:397–403 **(in Chinese with English abstract)**

Li Z, Chen B, Liu JW, Zhang L, Yang C (2015a) Zircon U–Pb ages and their implications for the South Liaohe Group in the Liaodong Peninsula, Northeast China. Acta Petrol Sin 31:1589–1605 **(in Chinese with English abstract)**

Li Z, Chen B, Wei CJ, Wang CX, Han W (2015b) Provenance and tectonic setting of the Paleoproterozoic metasedimentary rocks from the Liaohe Group, Jiao-Liao-Ji Belt, North China Craton: insights from detrital zircon U–Pb geochronology, whole-rock Sm–Nd isotopes, and geochemistry. J Asian Earth Sci 111:711–732

Li Z, Chen B, Wang JL (2016a) Geochronological framework and geodynamic implications of mafic magmatism in the Liaodong Peninsula and adjacent regions, North China Craton. Acta Geol Sin 90:138–153

Li Z, Chen B, Wei CJ (2016b) Hadean detrital zircon in the North China Craton. J Mineral Petrol Sci. doi:10.2465/jmps.150929

Lin Q, Wu FY, Liu SW, Ge WC, Sun JG, Yin JZ (1992) Archean granites in Eastern North China Craton. Science Press, Beijing, p 220 **(in Chinese with English abstract)**

Lin BX, Cui WY, Wang SQ, Shen ES (1997) Archean geology and gold deposit in western Liaoning Province. Seismological Press, Beijing **(in Chinese)**

Liu DY, Nutman AP, Compston W, Wu JS, Shen QH (1992) Remnants of ≥3800 Ma crust in the Chinese part of the Sino-Korean Craton. Geology 20:339–342

Liu JD, Xiao RG, Zhang YF, Fan MH, Wang SZ, Jia YG, Wang G, Liu ZX (2012) Zircon SHRIMP U–Pb dating of the tourmalinites from boron-bearing series of borate deposits in Eastern Liaoning and its geological implications. Acta Geol Sin 86:118–130

Lu LZ (1996) The Precambrian metamorphic geology and tectonic evolution of the Jiao-Liao massif. J Jilin Univ (Earth Sci Edn) 26:25–32 **(in Chinese with English abstract)**

Lu XP (2004) Paleo–Mesoproterozoic magmatic events in Tonghua area. Jilin University, Ph.D. thesis, p 151 **(in Chinese with English abstract)**

Lu XP, Wu FY, Lin JQ, Sun DY, Zhang YB, Guo CL (2004a) Geochronological successions of the Early Precambrian granitic magmatism in southern Liaoning Peninsula and its constraints on tectonic evolution of the North China Craton. Chin J Geol 39:123–139 **(in Chinese with English abstract)**

Lu XP, Wu FY, Zhang YB, Zhao CB, Guo CL (2004b) Emplacement age and tectonic setting of the Paleoproterozoic Liaoji granites in Tonghua area, southern Jilin Province. Acta Petrol Sin 20:381–392 **(in Chinese with English abstract)**

Lu XP, Wu FY, Guo JH, Yin CJ (2005) Late Paleoproterozoic granitic magmatism and crustal evolution in Tonghua region, northeast China. Acta Petrol Sin 21:721–736 **(in Chinese with English abstract)**

Lu XP, Wu FY, Guo JH, Wilde SA, Yang JH, Liu XM, Zhang XO (2006) Zircon U–Pb geochronological constraints on the Paleoproterozoic crustal evolution of the Eastern block in the North China Craton. Precambr Res 146:138–164

Lukkari S, Holtz F (2007) Phase relations of a F-enriched peraluminous granite: an experimental study of the Kymi topaz granite stock, southern Finland. Contrib Mineral Petrol 153:273–288

Luo Y, Sun M, Zhao GC, Li SZ, Xu P, Ye K, Xia XP (2004) LA-ICP-MS U–Pb zircon ages of the Liaohe Group in the Eastern Block of the North China Craton: constraints on the evolution of the Jiao-Liao-Ji Belt. Precambr Res 134:349–371

Luo Y, Sun M, Zhao GC, Li SZ, Ayers JC, Xia XP, Zhang JH (2008) A comparison of U–Pb and Hf isotopic compositions of detrital zircons from the North and South Liaohe Groups: constraints on the evolution of the Jiao-Liao-Ji Belt, North China Craton. Precambr Res 163:279–306

Meng QR (2003) What drove late Mesozoic extension of the northern China–Mongolia tract. Tectonophysics 369:155–174

Meng E, Liu FL, Cui Y, Liu PH, Liu CH, Shi JR (2013a) Depositional ages and tectonic implications for the Kuandian South Liaohe Group in northeast Liaodong Peninsula, northeast China. Acta Petrol Sin 29:2465–2480 **(in Chinese with English abstract)**

Meng E, Liu FL, Liu JH, Liu PH, Cui Y, Liu CH, Yang H, Wang F, Shi JR, Kong QB, Lian T (2013b) Zircon U–Pb and Lu–Hf isotopic constraints on Archean crustal evolution in the Liaonan Complex of northeast China. Lithos 177:164–183

Meng E, Liu FL, Liu PH, Liu CH, Yang H, Wang F, Shi JR, Cai J (2014) Petrogenesis and tectonic significance of Paleoproterozoic meta–mafic rocks from central Liaodong Peninsula, northeast China: evidence from zircon U–Pb dating and in situ Lu–Hf isotopes, and whole-rock geochemistry. Precambr Res 247:92–109

Miao LC, Zhang FQ, Liu DY (2010) Zircon SHRIMP U–Pb dating for gabbro at Chaotiehe in the Haicheng area, eastern Liaoning. Chin Sci Bull 55:403–410

Middlemost EA (1994) Naming materials in the magma/igneous rock system. Earth Sci Rev 37:215–224

Miyashiro A (1975) Classification, characteristics, and origin of ophiolites. J Geol 83:249–281

Mullen ED (1983) TiO_2–MnO–P_2O_5: a minor element discriminant for basaltic rocks of oceanic environments and its implications for petrogenesis. Earth Planet Sci Lett 62:53–62

Palmer MR (1991) Boron isotope systematics of hydrothermal fluids and tourmalines: a synthesis. Chem Geol 94:111–121

Peccerillo A, Taylor AR (1976) Geochemistry of Eocene calc-alkaline volcanic rocks from the Kastamonu area, Northern Turkey. Contrib Miner Petrol 58:63–81

Pei FP, Xu WL, Yang DB, Yu Y, Wang W, Zhao QG (2011) Geochronology and geochemistry of Mesozoic mafic–ultramafic complexes in the southern Liaoning and southern Jilin provinces, NE China: constraints on the spatial extent of destruction of the North China Craton. J Asian Earth Sci 40:636–650

Peng QM, Palmer MR (1995) The Paleoproterozoic boron deposits in eastern Liaoning, China: a metamorphosed evaporate. Precambr Res 72:185–197

Peng QM, Palmer MR (2002) The Paleoproterozoic Mg and Mg–Fe borate deposits of Liaoning and Jilin Provinces, Northeast China. Econ Geol 97:93–108

Peng P, Guo JH, Zhai MG, Bleeker W (2010) Paleoproterozoic gabbronoritic and granitic magmatism in the northern margin of the

North China craton: evidence of crust–mantle interaction. Precambr Res 183:635–659

Peng P, Guo JH, Windley BF, Li XH (2011) Halaqin volcano-sedimentary succession in the central–northern margin of the North China Craton: products of Late Paleoproterozoic ridge subduction. Precambr Res 187:165–180

Ryan JG, Langmuir CH (1993) The systematics of boron abundances in young volcanic-rocks. Geochim Cosmochim Acta 57:1489–1498

Santosh M (2010) Assembling North China Craton within the Columbia supercontinent: the role of double-sided subduction. Precambr Res 178:149–167

Santosh M, Wilde SA, Li JH (2007) Timing of Paleoproterozoic ultra high temperature metamorphism in the North China Craton: evidence from SHRIMP U–Pb zircon geochronology. Precambr Res 159:178–196

Simonen A (1953) Stratigraphy and sedimentation of the Svecofennidie, early Archean supracrustal rocks in southwestern Finland. Bull Geol Soc Finl 160:1–64

Slack JF, Palmer MR, Stevens BPJ, Barnes RG (1993) Origin and significance of tourmaline-rich rocks in the Broken Hill District, Australia. Econ Geol 88:505–541

Smith TE (1992) Volcanic rocks of early proterozoic greenstone belts, in proterozoic crustal evolution. In: Condie KC (ed) Proterozoic crustal evolution. Elsevier, Amsterdam, pp 1–54

Song B, Nutman AP, Liu DY, Wu JS (1996) 3800–2500 Ma crust in the Anshan area of Liaoning Province, northeastern China. Precambr Res 78:79–94

Sun M, Armstrong RL, Lambert RS, Jiang CC, Wu JH (1993) Petrochemistry and Sr, Pb and Nd isotopic geochemistry of Palaeoproterozoic Kuandian Complex, the eastern Liaoning province, China. Precambr Res 62:171–190

Sun M, Zhang LF, Wu JH (1996) The origin of the early Proterozoic Kuandian Complex: evidence from geochemistry. Acta Geol Sin 70:207–222 **(in Chinese with English abstract)**

Swihart GH, Moore PB, Callis EL (1986) Boron isotopic composition of marine and non-marine evaporite borates. Geochim Cosmochim Acta 50:1297–1301

Tam PY, Zhao GC, Liu FL, Zhou XW, Sun M, Li SZ (2011) Timing of metamorphism in the Paleoproterozoic Jiao-Liao-Ji Belt: new SHRIMP U–Pb zircon dating of granulites, gneisses and marbles of the Jiaobei massif in the North China Craton. Gondwana Res 19:150–162

Tam PY, Zhao GC, Sun M, Li SZ, Iizuka Y, Ma GS, Yin CQ, He YH, Wu ML (2012a) Metamorphic P–T path and tectonic implications of medium-pressure pelitic granulites from the Jiaobei massif in the Jiao-Liao-Ji Belt, North China Craton. Precambr Res 220–221:177–191

Tam PY, Zhao GC, Zhou XW, Sun M, Guo JH, Li SZ, Yin CQ, Wu ML, He YH (2012b) Metamorphic P–T path and implications of high-pressure politic granulites from the Jiaobei massif in the Jiao-Liao-Ji Belt, North China Craton. Gondwana Res 22:104–117

Tang HS, Wu G, Lai Y (2009) The C–O isotope geochemistry and genesis of the Dashiqiao magnesite deposit, Liaoning Province, NE China. Acta Petrol Sin 25:455–467 **(in Chinese with English abstract)**

Wan YS, Liu DY, Song B, Wu JS, Yang CH, Zhang ZQ, Geng YS (2005) Geochemical and Nd isotopic compositions of 3.8 Ga meta-quartz dioritic and trondhjemitic rocks from the Anshan area and their geological significance. J Asian Earth Sci 24:563–575

Wan YS, Song B, Liu DY, Wilde SA, Wu JS, Shi YR, Yin XY, Zhou HY (2006a) SHRIMP U–Pb zircon geochronology of Paleoproterozoic metasedimentary rocks in the North China Craton: evidence for a major Late Paleoproterozoic tectonothermal event. Precambr Res 149:249–271

Wan YS, Wilde SA, Liu DY, Yang CX, Song B, Yin XY (2006b) Further evidence for ~1.85 Ga metamorphism in the central zone of the North China Craton: SHRIMP U–Pb dating of zircons from metamorphic rocks in the Lushan area, Henan Province. Gondwana Res 9:189–197

Wan YS, Liu DY, Nutman A, Zhou HY, Dong CY, Yin XY, Ma MZ (2012) Multiple 3.8–3.1 Ga tectono-magmatic events in a newly discovered area of ancient rocks (the Shengousi Complex), Anshan, North China Craton. J Asian Earth Sci 54–55:18–30

Wan YS, Zhang YH, Williams IS, Liu DY, Dong CY, Fan RL, Shi YR, Ma MZ (2013) Extreme zircon O isotopic compositions from 3.8 to 2.5 Ga magmatic rocks from the Anshan area, North China Craton. Chem Geol 352:108–124

Wang XZ, Han X (1989) A study on metallogenic regularity of boron deposits in the Ji'an area, Jinlin Province. Jilin Geol 4:72–75 **(in Chinese)**

Wang GH, Zhang CH, Wang GS, Wu ZW (2001) Tectonic framework of Western Liaoning province and its evolution during Mesozoic. Geoscience 15:1–7 **(in Chinese with English abstract)**

Wang CZ, Xiao RG, Liu JD (2008) Ore-controlling factors and metallogenesis of borate deposits in eastern Liaoning and southern Jilin. Miner Depos 27:727–741 **(in Chinese with English abstract)**

Wang HC, Lu SN, Chu H, Xiang ZQ, Zhang CJ, Liu H (2011a) Zirocn U–Pb age and tectonic setting of meta-basalts of Liaohe Group in Helan area, Liaoyang, Liaoning Province. J Jilin Univ (Earth Sci Edn) 41:1321–1334 **(in Chinese with English abstract)**

Wang W, Liu SW, Bai X, Yang PT, Li QG, Zhang LF (2011b) Geochemistry and zircon U–Pb–Hf isotopic systematics of the Neoarchean Yixian-Fuxin greenstone belt, northern margin of the North China Craton: implications for petrogenesis and tectonic setting. Gondwana Res 20:64–81

Whalen JB, Currie KL, Chappell BW (1987) A-type granites: geochemical characteristics, discrimination and petrogenesis. Contrib Miner Petrol 95:407–419

Wilson W (1989) Igneous petrogenesis. Unwin Hyman, London, pp 327–373

Windley BF (1992) Proterozoic collisional and accretionary orogens. In: Condie KC (ed) Proterozoic crustal evolution. Elsevier, Amsterdam, pp 419–446

Wu FY, Ge WC, Sun DY, Lin Q, Zhou Y (1997) The Sm–Nd, Rb–Sr isotopic ages of the Archean granites in southern Jilin Province. Acta Petrol Sin 13:499–506 **(in Chinese with English abstract)**

Wu ZP, Hou XB, Li W (2007) Discussion on Mesozoic basin patterns and evolution in the eastern North China Block. Geotect Metall 31:385–399 **(in Chinese with English abstract)**

Xia XP, Sun M, Zhao GC, Luo Y (2006) LA–ICP–MS U–Pb geochronology of detrital zircons from the Jining Complex, North China Craton and its tectonic significance. Precambr Res 144:199–212

Xie LW, Yang JH, Wu FY, Yang YH, Wilde SA (2011) PbSL dating of garnet and staurolite: constraints on the Paleoproterozoic crustal evolution of the Eastern Block, North China Craton. J Asian Earth Sci 42:142–154

Yan XL, Chen B (2014) Chemical and boron isotope compositions of tourmaline from the Paleoproterozoic Houxianyu borate deposit, NE China: implications for the origin of borate deposit. J Asian Earth Sci 94:252–266

Yang JH, Wu FY, Xie LW, Liu XM (2007) Petrogenesis and tectonic implications of Kuangdonggou synites in the Liaodong Peninsula, east North China Craton: constraints from in-suit zircon U–Pb ages and Hf isotopes. Acta Petrol Sin 23:263–276 **(in Chinese with English abstract)**

Yang MC, Chen B, Yan C (2015a) Petrogenesis and their tectonic implications of the Paleoproterozoic gneissic granites from

Jiao-Liao-Ji Belt, North China Craton. J Earth Sci Environ 7:1–9 **(in Chinese with English abstract)**

Yang MC, Chen B, Yan C (2015b) Petrological, geochronological, geochemical and Sr–Nd–Hf isotopic constraints on the petrogenesis of the Shuangcha Paleoproterozoic megaporphyritic granite in the southern Jilin Province: tectonic implications. Acta Petrol Sin 31:1573–1588 **(in Chinese with English abstract)**

Yin A, Nie S (1996) Phanerozoic palinspastic reconstruction of China and its neighboring regions. In: Yin A, Harrison TM (eds) The tectonic evolution of asia. Cambridge University Press, New York, pp 285–442

Yu JJ, Yang DB, Feng H, Lan X (2007) Chronology of amphibolite protolith in Haicheng of southern Liaoning: evidence from LA–ICP–MS zircon U–Pb dating. Glob Geol 26:391–407 **(in Chinese with English abstract)**

Yuan LL, Zhang XH, Zhai MG (2015) Two episodes of Paleoproterozoic mafic intrusions from Liaoning province, North China Craton: petrogenesis and tectonic implications. Precambr Res 264:119–139

Zhai MG, Santosh M (2011) The early Precambrian odyssey of North China Craton: a synoptic overview. Gondwana Res 20:6–25

Zhai MG, Santosh M (2013) Metallogeny of the North China Craton: link with secular changes in the evolving Earth. Gondwana Res 24:275–297

Zhang JS (1994) Mineral deposits and mineralization of szaibelyite boron deposits, eastern Liaoning province. Liaoning Geol 4:289–303 **(in Chinese)**

Zhang QS, Yang ZS (1988) Early crust and mineral deposits of Liaodong Peninsula. Geological Publishing House, Beijingm, pp 218–450 **(in Chinese with English abstract)**

Zhang SH, Zhao Y, Yang ZY, He ZF, Wu H (2009) The 1.35 Ga diabase sills from the northern North China Craton: implications for breakup of the Columbia (Nuna) supercontinent. Earth Planet Sci Lett 288:588–600

Zhang YF, Liu JD, Xiao RG, Wang SZ, Wang J, Bao DJ (2010) The Hyalotourmalites of Houxianyu Borate Deposit in Eastern Liaoning: zircon Features and SHRIMP Dating. Earth Science J China Univ Geosci 35:985–999

Zhang SH, Zhao Y, Santosh M (2012) Mid-Mesoproterozoic bimodal magmatic rocks in the northern North China Craton: implications for magmatism related to breakup of the Columbia supercontinent. Precambr Res 222–223:339–367

Zhao GC, Zhai MG (2013) Lithotectonic elements of Precambrian basement in the North China Craton: review and tectonic implications. Gondwana Res 23:1207–1240

Zhao GC, Sun M, Wilde SA, Li SZ (2005) Late Archean to Paleoproterozoic evolution of the North China Craton: key issues revisited. Precambr Res 136:177–202

Zhao GC, Wilde SA, Guo JH, Cawood PA, Sun M, Li XP (2010) Single zircon grains record two Paleoproterozoic collisional events in the North China Craton. Precambr Res 177:266–276